

**Supplementary information**

---

**A 9.2-GHz clock transition in a Lu(II) molecular spin qubit arising from a 3,467-MHz hyperfine interaction**

---

In the format provided by the authors and unedited

# Supplementary Information for

## 9.2 GHz clock transition in a Lu(II) molecular spin qubit arising from a 3467 MHz hyperfine interaction

Krishnendu Kundu, Jessica R. K. White, Samuel A. Moehring, Jason M. Yu, Joseph W. Ziller, Philipp Furche, William J. Evans and Stephen Hill

Correspondence to: [filipp.furche@uci.edu](mailto:filipp.furche@uci.edu), [wevans@uci.edu](mailto:wevans@uci.edu), [shill@magnet.fsu.edu](mailto:shill@magnet.fsu.edu)

### Contents

1. Structural Characterization	2
2. Synthetic Details	7
3. EPR Simulations	13
4. Spin-Lattice Relaxation Time ( $T_1$ ) Measurements	17
5. Computational Details	17
6. Crystallography	20
7. References	21
Tables 7 to 14	25
CheckCIF reports	60

## 1. Structural Characterization

$\text{Lu}(\text{OAr}^*)_3$  crystallizes in the  $P2_1/n$  space group (Table 1)<sup>1</sup> and has similar unit cell constants as the previously reported  $\text{Y}(\text{OAr}^*)_3$ .<sup>2</sup> Like the Y analogue,  $\text{Lu}(\text{OAr}^*)_3$  is pseudo- $C_3$  symmetric, and the geometry about the Lu atom is slightly pyramidalized with the Lu atom displaced from the  $\text{O}_3$  plane by 0.500 Å (Fig. 1).  $[\text{K}(\text{crypt})][\text{Lu}(\text{OAr}^*)_3]$  (**4**) crystallizes in the  $P\bar{1}$  space group (Table 2)<sup>1</sup> and is isomorphous with  $[\text{K}(\text{crypt})][\text{Y}(\text{OAr}^*)_3]$ .<sup>2</sup> Interestingly, **4** is only the second crystallographically characterized Lu(II) complex, the other being  $[\text{K}(\text{crypt})][\text{Cp}'_3\text{Lu}]$  ( $\text{Cp}' = \text{C}_5\text{H}_4\text{SiMe}_3$ ).<sup>3</sup> Like the Y analogue, **4** is more planar than the Lu(III) precursor (Fig. 2): the Lu center is only 0.147 Å above the  $\text{O}_3$  plane. The average of the 2.062(2), 2.069(2), and 2.074(2) Å Lu-O distances in **4** is 0.056 Å larger than the average of the 2.002(2), 2.014(2), and 2.020(2) Å Lu-O lengths in  $\text{Lu}(\text{OAr}^*)_3$ . The analogous difference in the yttrium analogs is 0.06 Å.<sup>2</sup> Differences less than 0.1 Å are typical when comparing  $4f^n \text{Ln}(\text{III})$  and  $4f^{n-1}5d^1 \text{Ln}(\text{II})$  ions.<sup>2</sup>

**Table 1:** Crystal data and structure refinement for Lu(OAr\*)<sub>3</sub> (CCDC 2074947).<sup>1</sup>

Empirical formula	C <sub>96</sub> H <sub>137</sub> Lu O <sub>3</sub>
Formula weight	1514.02
Temperature	133(2) K
Wavelength	0.71073 Å
Crystal system	Monoclinic
Space group	<i>P</i> 2 <sub>1</sub> / <i>n</i>
Unit cell dimensions	$a = 14.7454(12) \text{ \AA}$ $\alpha = 90^\circ$ $b = 29.237(2) \text{ \AA}$ $\beta = 108.8157(13)^\circ$ $c = 22.0531(18) \text{ \AA}$ $\gamma = 90^\circ$
Volume	8999.3(13) Å <sup>3</sup>
Z	4
Density (calculated)	1.117 Mg/m <sup>3</sup>
Absorption coefficient	1.142 mm <sup>-1</sup>
F(000)	3232
Crystal color	colorless
Crystal size	0.569 x 0.386 x 0.295 mm <sup>3</sup>
Theta range for data collection	1.199 to 28.282°
Index ranges	-19 ≤ <i>h</i> ≤ 19, -38 ≤ <i>k</i> ≤ 38, -29 ≤ <i>l</i> ≤ 29
Reflections collected	201896
Independent reflections	22343 [R(int) = 0.0578]
Completeness to theta = 25.242°	100.0 %
Absorption correction	Semi-empirical from equivalents
Max. and min. transmission	0.7461 and 0.6554
Refinement method	Full-matrix least-squares on F <sup>2</sup>
Data / restraints / parameters	22343 / 18 / 912
Goodness-of-fit on F <sup>2</sup>	1.186
Final R indices [ <i>I</i> > 2σ( <i>I</i> ) = 19679 data]	R1 = 0.0468, wR2 = 0.1059
R indices (all data, 0.75 Å)	R1 = 0.0538, wR2 = 0.1086
Largest diff. peak and hole	2.229 and -4.477 e.Å <sup>-3</sup>

**Table 2:** Crystal data and structure refinement for [K(crypt)][Lu(OAr<sup>\*</sup>)<sub>3</sub>].3Et<sub>2</sub>O (**4** – CCDC 2074946).<sup>1</sup>

Empirical formula	C <sub>120</sub> H <sub>189</sub> K Lu N <sub>2</sub> O <sub>12</sub>
Formula weight	2065.79
Temperature	133(2) K
Wavelength	0.71073 Å
Crystal system	Triclinic
Space group	<i>P</i> $\bar{1}$
Unit cell dimensions	<i>a</i> = 16.3861(17) Å $\alpha$ = 84.5286(18)° <i>b</i> = 16.7674(17) Å $\beta$ = 82.7989(18)° <i>c</i> = 22.820(2) Å $\gamma$ = 62.6481(15)°
Volume	5519.9(10) Å <sup>3</sup>
Z	2
Density (calculated)	1.243 Mg/m <sup>3</sup>
Absorption coefficient	0.992 mm <sup>-3</sup>
F(000)	2218
Crystal color	purple
Crystal size	0.274 x 0.267 x 0.198 mm <sup>3</sup>
Theta range for data collection	1.369 to 28.282°
Index ranges	-21 ≤ <i>h</i> ≤ 21, -22 ≤ <i>k</i> ≤ 22, -30 ≤ <i>l</i> ≤ 30
Reflections collected	124026
Independent reflections	27368 [R(int) = 0.0633]
Completeness to theta = 25.242°	100.0 %
Absorption correction	Semi-empirical from equivalents
Max. and min. transmission	0.8017 and 0.7228
Refinement method	Full-matrix least-squares on F <sup>2</sup>
Data / restraints / parameters	27368 / 0 / 1240
Goodness-of-fit on F <sup>2</sup>	1.055
Final R indices [ <i>I</i> > 2σ( <i>I</i> ) = 22821 data]	R1 = 0.0465, wR2 = 0.1110
R indices (all data, 0.75 Å)	R1 = 0.0631, wR2 = 0.1183
Largest diff. peak and hole	4.488 and -0.890 e.Å <sup>-3</sup>

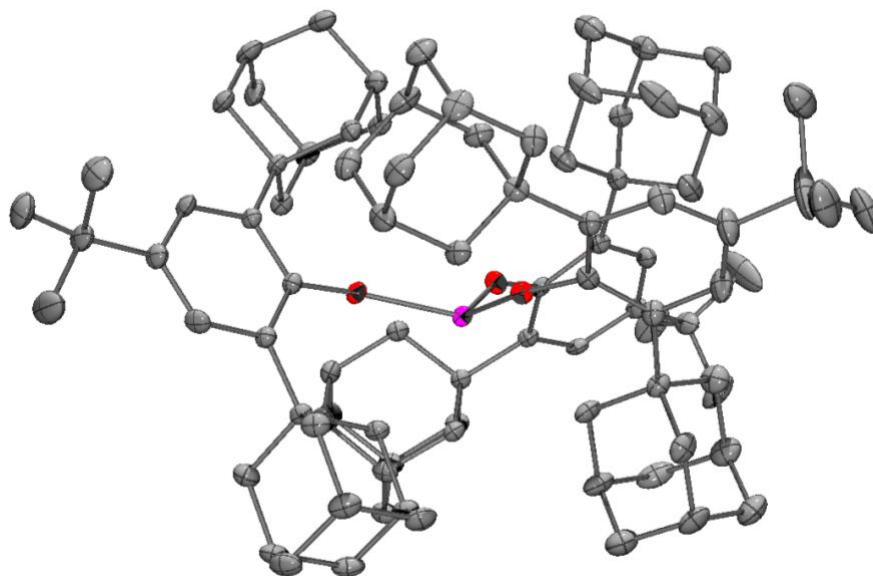


**Figure 1.** Thermal ellipsoid plot of Lu(OAr<sup>+</sup>)<sub>3</sub> drawn at the 50% probability level. One hexane solvent molecule and H atoms are omitted for clarity. Color code: Grey = C, Red = O, Pink = Lu.

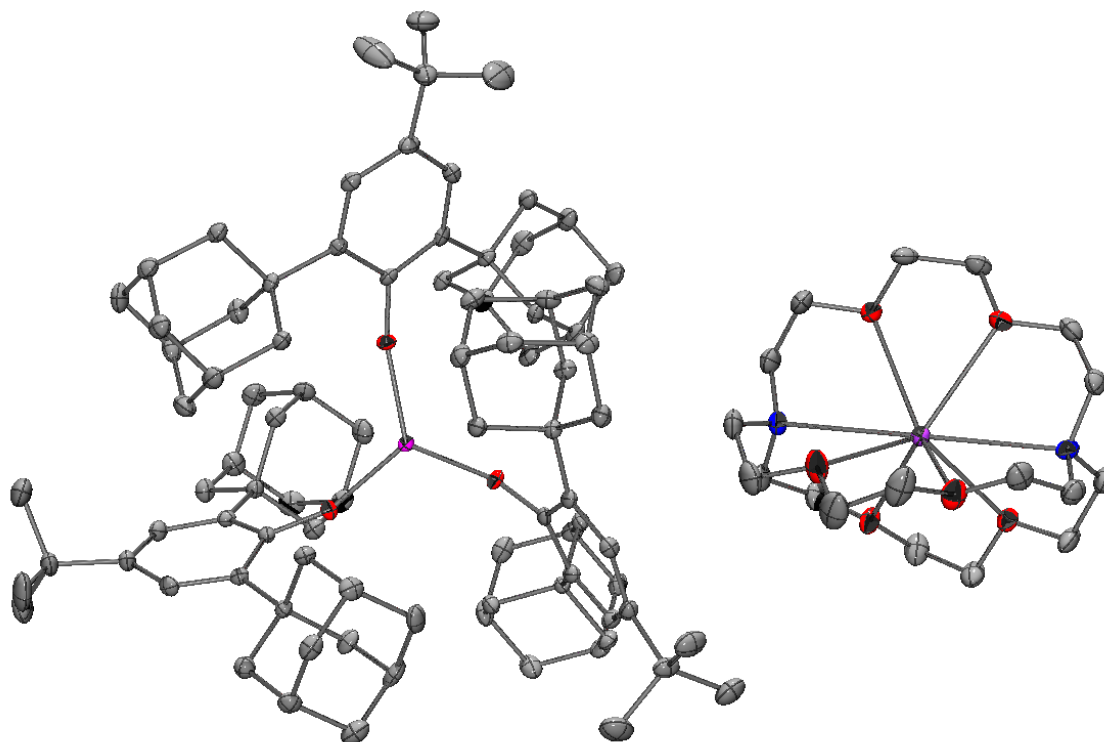


**Figure 2.** Thermal ellipsoid plot of [K(crypt)][Lu(OAr<sup>+</sup>)<sub>3</sub>] (**4**) drawn at the 50% probability level. Three ether solvent molecules and H atoms are omitted for clarity. Color code: Grey = C, Red = O, Blue = N, Pink = Lu.

Steric saturation about the metal center in Ln(III) and Ln(II) complexes plays an important role in their stability and isolation. Solid-G analysis by Guzei<sup>4</sup> was employed to quantify the degree of steric saturation about the Lu(III) and Lu(II) ions in Lu(OAr\*)<sub>3</sub> and [K(crypt)][Lu(OAr\*)<sub>3</sub>], respectively. The Solid-G program converts the calculated ligand solid angles into a percentage (the *G* parameter) to demonstrate how much of the coordination sphere of the metal center in an organometallic complex is shielded by its ligands. For instance, a percentage, or *G* value, of 100% indicates that the coordination sphere of the metal ion is fully saturated and its ligands completely shield the metal from an outside molecule, whereas a low *G* value indicates that the ligands only shield the metal by X%, leaving (100-X)% of the coordination sphere open for an outside molecule to reach the metal center.

**Table 3:** Selected structural parameters of Lu(OAr\*)<sub>3</sub> and [K(crypt)][Lu(OAr\*)<sub>3</sub>] (**4**) and comparison of *G* values of other rare-earth metal complexes.

Complex <sup>[Ref]</sup>	<i>G</i> [%]	$\delta$
Lu(OAr*) <sub>3</sub>	92	0.500
[K(crypt)][Lu(OAr*) <sub>3</sub> ]	91	0.147
Y(OAr*) <sub>3</sub> <sup>[2]</sup>	92	0.431
[K(crypt)][Y(OAr*) <sub>3</sub> ] <sup>[2]</sup>	90	0.125
Cp' <sub>3</sub> Lu <sup>[7]</sup>	88	
[K(crypt)][Cp' <sub>3</sub> Lu] <sup>[3]</sup>	88	
Cp <sup>tet</sup> <sub>3</sub> Lu <sup>[8]</sup>	87	
Lu(NR <sub>2</sub> ) <sub>3</sub> <sup>[9]</sup>	86	
Ln(OAr) <sub>3</sub> <sup>[10]</sup>	84	

$\delta$  is the displacement of Lu from the O<sub>3</sub> plane in Å. R = SiMe<sub>3</sub>, Cp<sup>tet</sup> = C<sub>5</sub>(CH<sub>3</sub>)<sub>4</sub>H, OAr = 2,6-di-*t*-butyl-phenoxide.

The *G* values of Lu(OAr\*)<sub>3</sub> and **4** were calculated to be 92% and 91%, respectively (Table 3). These *G* values are similar to those reported for Y(OAr\*)<sub>3</sub> (92%), and [K(crypt)][Y(OAr\*)<sub>3</sub>] (90%).<sup>2</sup> The aryloxy ligands in **4** greatly shield the Lu(II) ion, which may be a reason for its thermal stability. Compared to other Ln(II) complexes which

generally decompose rapidly at room temperature, **4** is stable at room temperature for at least 4 hours. Compared to other Lu(III) complexes,<sup>5-10</sup> Lu(OAr\*)<sub>3</sub> is the most sterically saturated. Lu(OAr)<sub>3</sub> (OAr = 2,6-di-*t*-butyl-phenoxide), another Lu aryloxy complex,<sup>10</sup> is noticeably less sterically saturating with a *G* value of 84%, suggesting that the adamantyl substituents on the aryloxy of Lu(OAr\*)<sub>3</sub> are important in shielding the Lu center. It is important to note that the maximization of *G* is not necessarily the best strategy for isolating Ln(II) complexes, as Solid-G analysis does not take the counteraction into effect, and the cation has shown to play an important role in the stability and isolation of Ln(II) complexes.<sup>11</sup> Also, different ligand sets seem to have their own optimum *G* value, so the most sterically saturated Ln(II) complex in a series is not necessarily the most stable.<sup>6</sup> However, even if steric saturation is not the most important factor in all ligand systems, the great amount of steric bulk that the adamantyl substituents provide in the OAr\* ligand seems to be important for the stability of Ln(II) aryloxy complexes.

## 2. Synthetic Details

*General:* All manipulations and syntheses described below were conducted with the rigorous exclusion of air and water using standard Schlenk line and glovebox techniques under an argon atmosphere, unless stated otherwise. Solvents were sparged with UHP argon and dried by passage through columns containing Q-5 and molecular sieves prior to use. Potassium bis(trimethylsilyl)amide (KNR<sub>2</sub>, R = SiMe<sub>3</sub>) (Aldrich, 98%), was dissolved in toluene, centrifuged to remove tacky yellow insoluble material, and solvent was removed under reduced pressure before use. 2.2.2-Cryptand (crypt, Merck) was placed under vacuum (10<sup>-5</sup> torr) for 12 h before use. Lu(NR<sub>2</sub>)<sub>3</sub><sup>12</sup> and HOAr<sup>Ad,Ad,t-Bu</sup> (HOAr\*)<sup>13</sup> were prepared according to the literature procedures. Deuterated NMR solvents were dried over NaK alloy, degassed by three freeze-pump-thaw cycles, and vacuum transferred before use. <sup>13</sup>C{<sup>1</sup>H} NMR spectra were obtained on a Bruker AVANCE600 spectrometer with a BBO probe operating at 150 MHz for <sup>13</sup>C at 298 K and referenced internally to residual protio-solvent resonances. <sup>1</sup>H NMR spectra were obtained on a Bruker CRYO500 MHz spectrometer with a TCI probe at 25 °C and referenced internally to residual protio-solvent resonances. UV/Vis spectra were collected in THF at 298 K using a Varian Cary 50 Scan UV/Vis spectrophotometer. Infrared (IR) transmittance measurements were taken as compressed solids on an Agilent Cary 630



FTIR spectrophotometer with a diamond ATR attachment. Complexes **2** and **3** were prepared in analogy to the preparation of **4**, which is detailed below.

$\text{Lu}(\text{OAr}^{\text{Ad,Ad,t-Bu}})_3$ :  $\text{Lu}(\text{OAr}^{\text{Ad,Ad,t-Bu}})_3$  [ $\text{Lu}(\text{OAr}^*)_3$ ] was synthesized using modified procedures reported for  $\text{Y}(\text{OAr}^*)_3$ .<sup>2</sup> In an argon glovebox,  $\text{Lu}(\text{NR}_2)_3$  (625 mg, 0.953 mmol),  $\text{HOAr}^*$  (998 mg, 2.38 mmol), and toluene (50 mL) were added to a 100 mL Schlenk flask fitted with a Teflon stopper. The flask was taken out of the glovebox and connected to a Schlenk line. The clear reaction solution was heated to 100 °C using an oil bath. After stirring for two days at 100 °C, the flask was briefly opened to vacuum to release vapor (presumably toluene and/or  $\text{HNR}_2$ ). The reaction was stirred at 100 °C under reduced pressure for an additional 2 days. The reaction was then slowly concentrated to 15 mL and changed from colorless to pale-yellow. The reaction flask was brought back into an argon-filled glovebox and the pale-yellow solution was transferred to a 20 mL scintillation vial. After a few days in a -35 °C freezer, a colorless precipitate formed along the walls of the vial. The yellow toluene solution was decanted from the colorless precipitate and the precipitate was washed with pentane, yielding  $\text{Lu}(\text{OAr}^*)_3$  as a bright white powder. Single crystals suitable for X-ray diffraction were grown from boiling hexane. NMR, IR, and UV-visible spectra are shown in Figs. 3–6.  $^1\text{H}$  NMR ( $\text{C}_6\text{D}_6$ ):  $\delta$  7.35 (s, 6H) 2.51 (d,  $J = 11.1$  Hz, 18H), 2.39 (d,  $J = 11.0$  Hz, 18H), 2.05 (s, 18H), 1.74 (d,  $J = 12.9$  Hz, 18H), 1.65 (d,  $J = 12.0$  Hz, 18H), 1.42 (s, 27H, *t-Bu*).  $^{13}\text{C}\{^1\text{H}\}$  NMR ( $\text{C}_6\text{D}_6$ ):  $\delta$  142.02, 139.34, 136.11, 135.65, 122.57, 44.41, 39.12, 37.35, 34.70, 32.11, 29.80. IR: 3631br, 2899str, 2846str, 2676w, 2654w, 1445m, 1428m, 1390w, 1359w, 1342w, 1312w, 1278m, 1241m, 1202w, 1170w, 1135w, 1100w, 1078w, 1034w, 978 w, 922 w, 900w, 872m, 845m, 817w, 766w, 710w  $\text{cm}^{-1}$ . Anal. Calcd for  $(\text{C}_{90}\text{H}_{123}\text{O}_3\text{Lu})\cdot(\text{C}_6\text{H}_{14})$ : C, 76.15; H, 9.12. Found: C, 74.02; H, 8.88. The found values (74.02, 8.88), formulate to be  $\text{C}_{96}\text{H}_{137}$ , which matches the calculated formula  $\text{C}_{96}\text{H}_{137}$  for crystalline  $\text{Lu}(\text{OAr}^*)_3$  with one molecule of hexane present. The analytical data are not consistent with contamination of the sample with  $\text{HOAr}^*$ . Incomplete combustion during elemental analysis is a well-reported issue within rare-earth metal chemistry,<sup>14-18</sup> and other reported rare-earth metal aryloxide complexes also have a low %C value.<sup>2,6,19</sup>

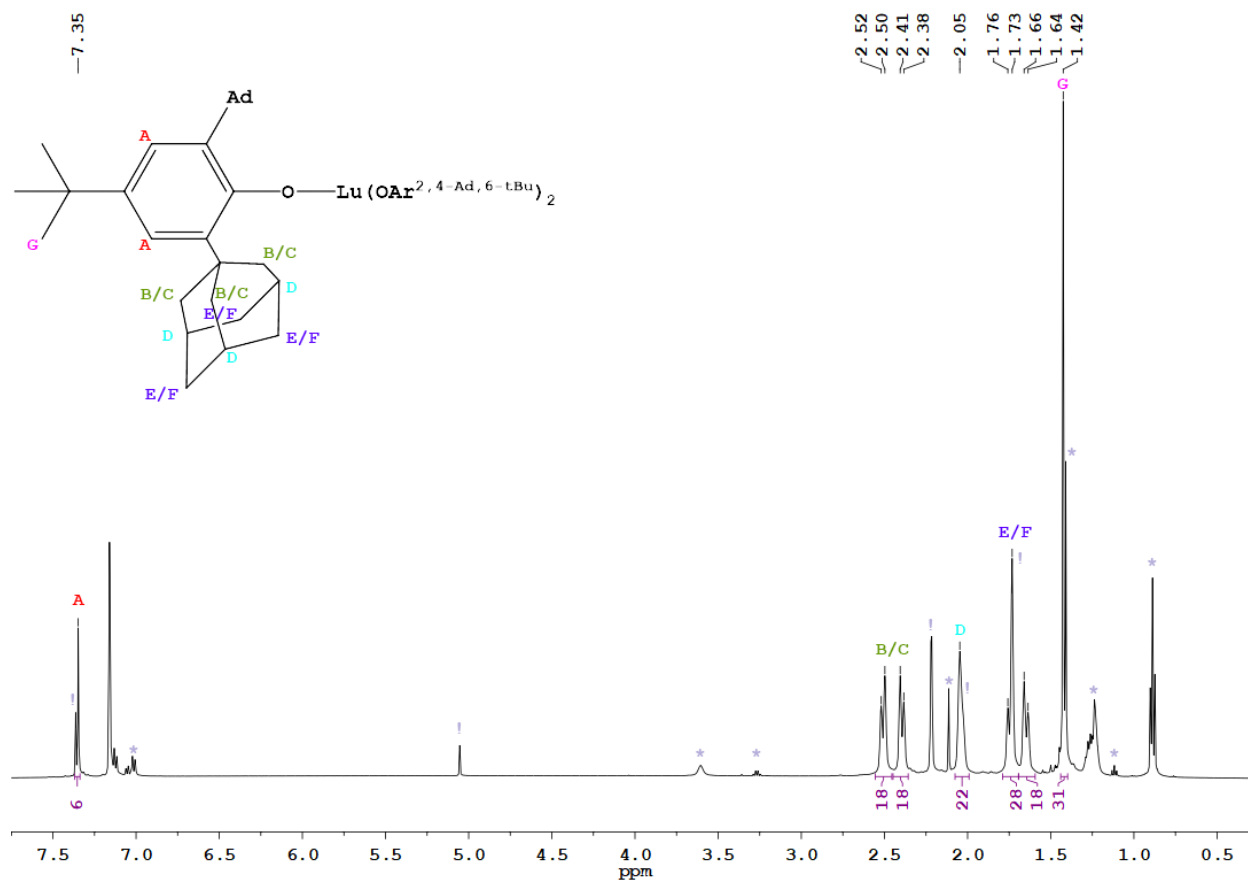


**Figure 3.**  $^1\text{H}$  NMR spectrum of  $\text{Lu}(\text{OAr}^*)_3$ . Peaks marked with ‘!’ originate from residual  $\text{HOAr}^*$  and those marked with ‘\*’ originate from residual solvent.

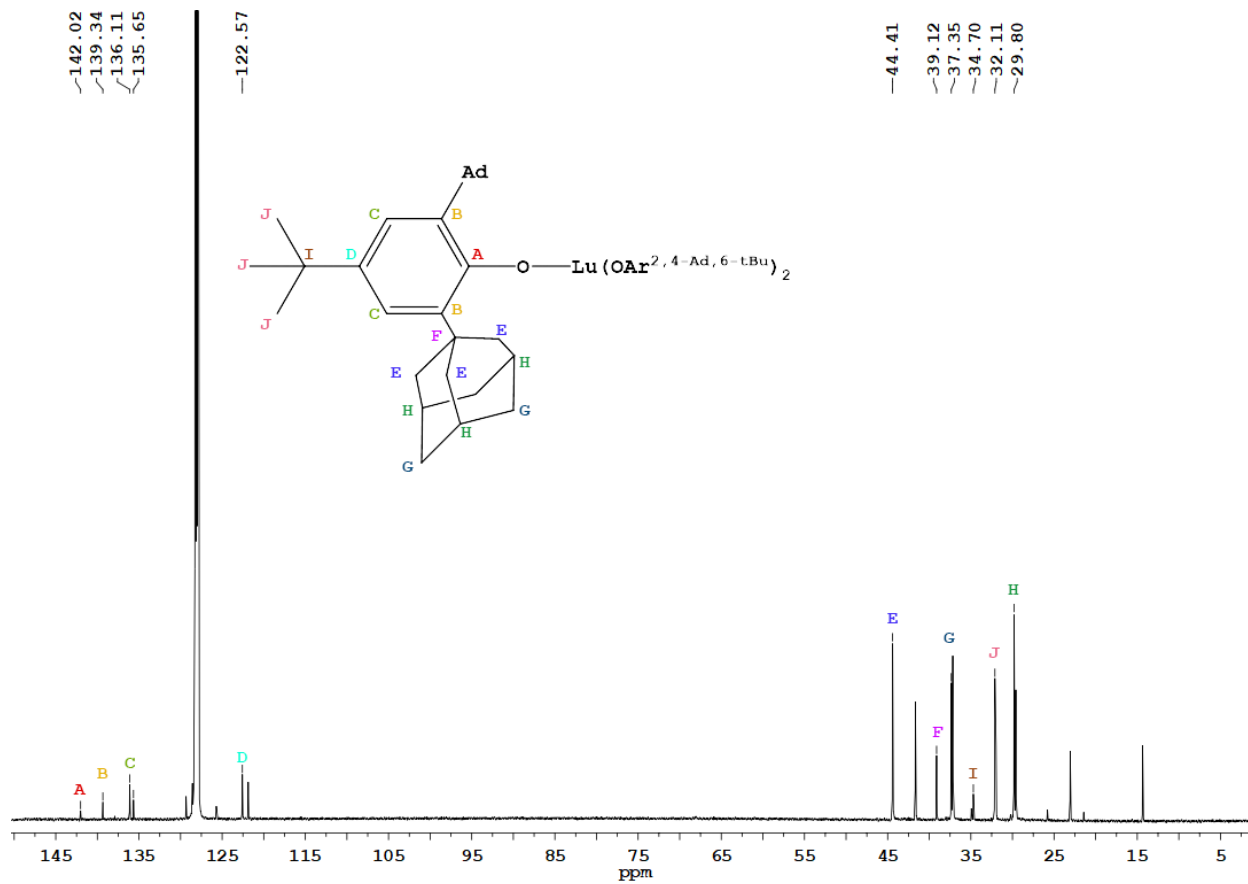


**Figure 4.**  $^{13}\text{C}\{^1\text{H}\}$  NMR spectrum of  $\text{Lu}(\text{OAr}^*)_3$ . Unmarked peaks originate from residual solvent.

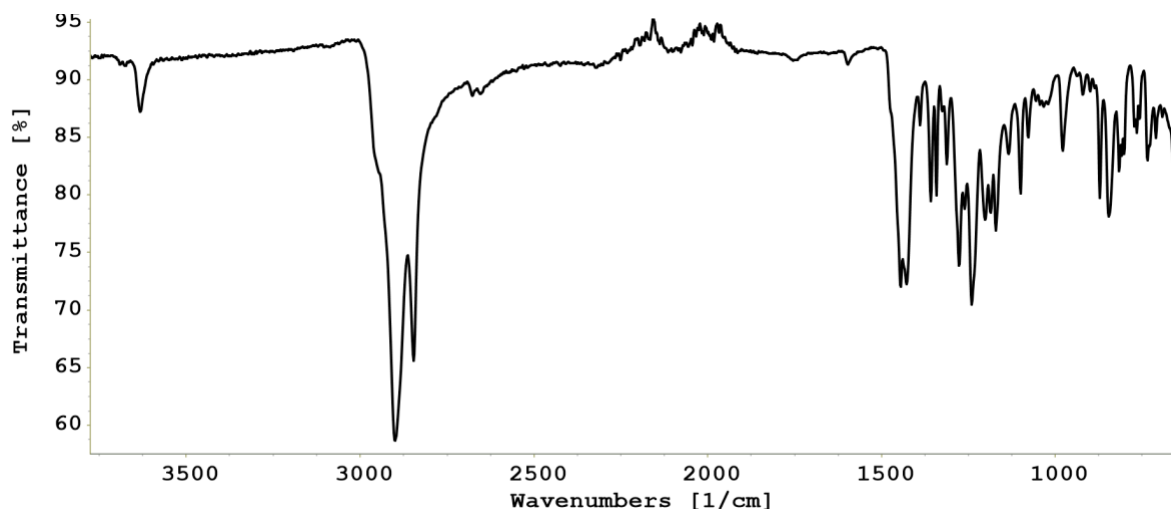


**Figure 5.** IR spectrum of  $\text{Lu}(\text{OAr}^*)_3$  solids with residual  $\text{HOAr}^*$  present. Recrystallization is necessary to remove all traces of  $\text{HOAr}^*$  as it persists through multiple washings of  $\text{Lu}(\text{OAr}^*)_3$  solids with pentane.

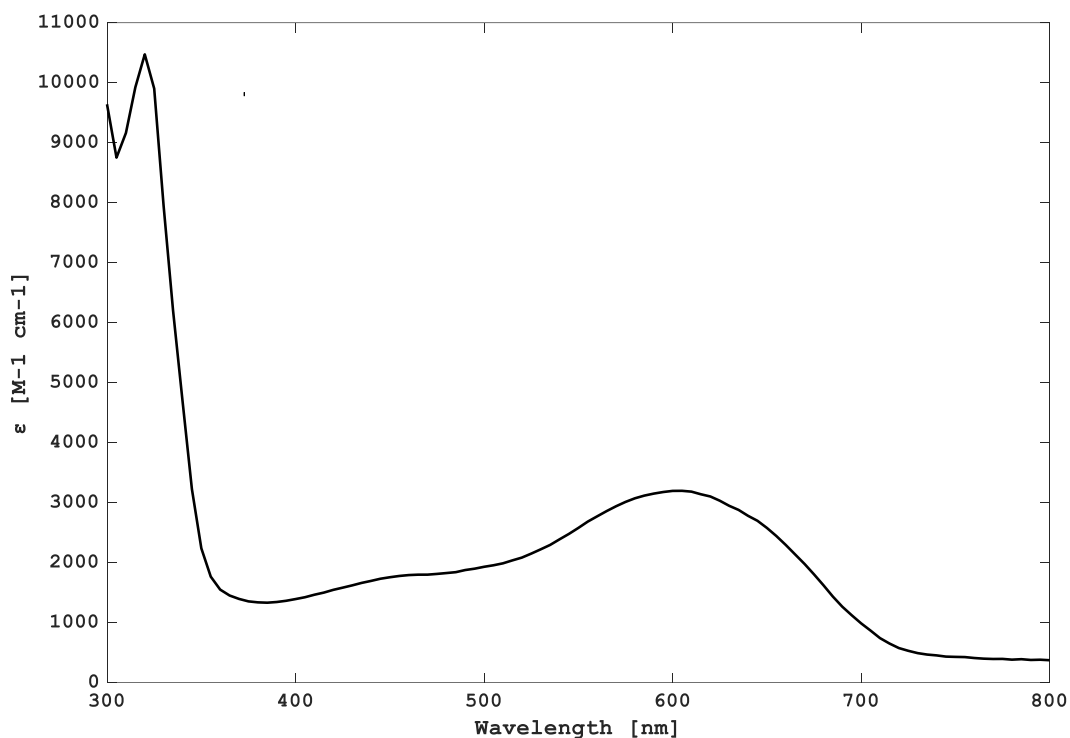


**Figure 6.** UV/vis spectrum of a 1 mM THF solution of  $[\text{K}(\text{crypt})][\text{Lu}(\text{OAr}^*)_3]$  (**4**) collected at RT.

*[K(crypt)][Lu(OAr\*)<sub>3</sub>]* (**4**): A mixture of Lu(OAr\*)<sub>3</sub> (80 mg, 0.056 mmol) and crypt (21 mg, 0.056 mmol) in 5 mL Et<sub>2</sub>O was chilled to -35 °C and then added to a vial containing chilled (-35 °C) KC<sub>8</sub> (10 mg, 0.067 mmol). The cloudy colorless mixture instantly turned dark blue. After 1 hour at -35 °C with occasional swirling, the KC<sub>8</sub> was filtered from the dark blue solution using a Kimwipe-packed glass pipette. The solvent was slowly removed *in vacuo* to yield dark blue X-ray quality single crystals of [K(crypt)][Lu(OAr\*)<sub>3</sub>].3Et<sub>2</sub>O. THF and a potassium smear were used instead of Et<sub>2</sub>O and KC<sub>8</sub> when preparing samples of [K(crypt)][Lu(OAr\*)<sub>3</sub>] *in situ* for EPR measurements. UV/Vis  $\lambda_{\max}$  ( $\epsilon$ , THF, RT): 456 nm (shoulder, 1777 M<sup>-1</sup> cm<sup>-1</sup>), 605 nm (3197 M<sup>-1</sup> cm<sup>-1</sup>).

*General protocol for preparation of samples for EPR measurements:* With a soldering iron, holes were made through a 1.5 mL Eppendorf tube and a 50 mL Falcon tube and cap so that they easily submerge under liquid nitrogen (Fig. 7). LuA<sub>3</sub> (A = N(SiMe<sub>3</sub>)<sub>2</sub>, OAr\*) and crypt were dissolved in the appropriate amount of THF to result in final Lu(II) concentrations of approximately 1 mM, 5 mM, 10 mM and 20 mM.

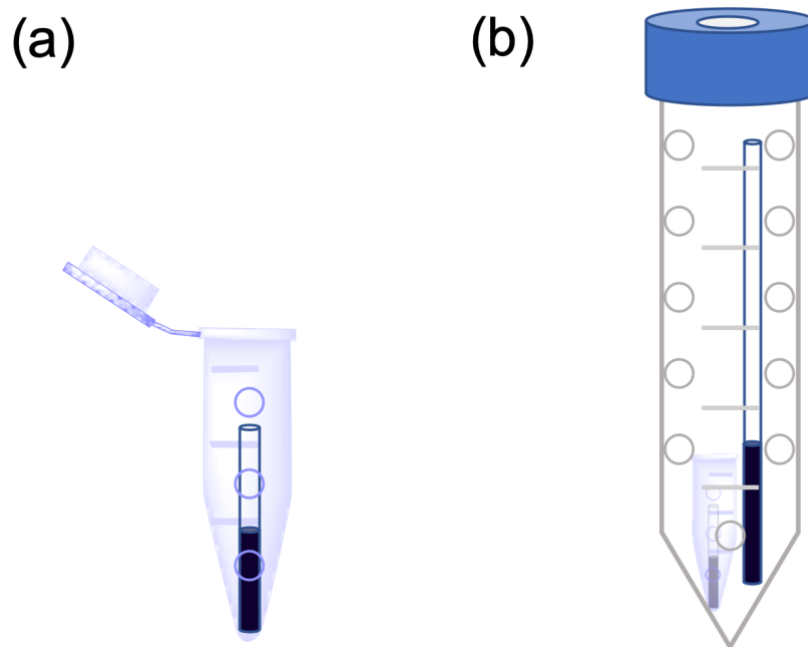


**Figure 7.** A depiction of (a) the Eppendorf tube holding the W-band EPR sample and (b) the 50 mL Falcon tube holding both W-band and X-band EPR samples.

In an argon-filled glovebox, a Wilmad quartz 100 mm tube for X-band EPR, a custom-made plastic W-band EPR tube contained in the Eppendorf tube, a vial containing the

THF solution of LuA<sub>3</sub> and crypt, a vial containing an excess (>10 eq) of potassium smear, and several glass pipettes, one of which had a Kimwipe packed into it, were placed in a cold well and were allowed to cool to -78 °C. The THF solution of LuA<sub>3</sub> and crypt was added to the vial containing the potassium smear. Upon swirling the vial, a gradual change in color from colorless to dark blue was observed. After 1 hour at -78 °C, the dark blue THF solution containing [K(crypt)][LuA<sub>3</sub>] was filtered. An aliquot was placed in the W-band tube (still in the Eppendorf) so that the tube was approximately half filled, and then the Eppendorf tube was capped. An aliquot was placed in the X-band tube so that the sample height was 1.5 cm, and then the tube was capped. Both tubes were quickly placed in a chilled beaker containing chilled Lab Armor metal beads so that both tubes were upright and stable. This beaker was immediately taken out of the glovebox, the Eppendorf and X-band tubes were uncapped, and the samples were immediately frozen in liquid nitrogen. Both tubes were then placed in a prechilled 50 mL Falcon tube (Fig. 7). The Falcon tube was then capped and submerged in liquid nitrogen inside of a shipping Dewar.

### 3. EPR Simulations

*Electron-nuclear hyperfine splitting pattern:* Two factors dominate the main trends seen in the high-field EPR spectra (Fig. 3, main article): *g*-tensor anisotropy and the hyperfine interaction. This is qualitatively illustrated with the aid of the simulations displayed in Extended Data Fig. 1a for compounds **2** and **4**. In the absence of a hyperfine interaction, the shape of the spectrum is dictated by the axial  $\vec{g}$ -tensor and the molecular orientational distribution in the solution. Assuming  $g_x = g_y < g_z$ , as is approximately the case for compounds **2** to **4**, then  $g(\theta) = (g_z^2 \cos^2 \theta + g_x^2 \sin^2 \theta)^{1/2}$ , where  $\theta$  denotes the orientation of the local molecular z-axis relative to the applied field. The derivative of this function,  $dg(\theta)/d\theta = -(g_z^2 - g_x^2) \sin \theta \cos \theta / g(\theta)$ , resulting in turning points in the solution EPR spectrum at  $\theta = 0$  and  $90^\circ$ , where  $g(\theta)$  does not vary with molecular orientation (i.e.,  $dg/d\theta = 0$ ). Thus,  $g(\theta)$  is a continuous function that spans from  $g_x$  to  $g_z$ , resulting in electron spin echo (ESE) intensity from  $B_{0\parallel} = hf/g_z\mu_B$  to  $B_{0\perp} = hf/g_x\mu_B$ . More importantly, the inverse derivative,  $d\theta/dg$ , diverges at both  $\theta = 0$  and  $90^\circ$  and, therefore, at  $B_{0\parallel}$  and  $B_{0\perp}$ ;  $d\theta/dg$  is proportional to the range of molecular orientations that contribute

to a given range of  $g$ -values. To fully understand the line shape, one must also evaluate the orientational density-of-states (DOS),  $dN/d\theta \propto \sin \theta$ , where  $dN$  is the number of molecules in the angle range  $d\theta$ , i.e., the orientational DOS vanishes at the poles ( $B_0 \parallel z$ ) and is maximum at the equator ( $B_0 \perp z$ ). The product,  $dN/d\theta \times d\theta/dg = dN/dg$ , then gives the number of molecules contributing to a given portion of the ESE spectrum. As can be seen, the cancelation of  $\sin \theta$  means that  $dN/dg$  diverges only at  $\theta = 90^\circ$ , dictated by  $g_{xy}$ . Therefore, upon sweeping from low to high field, there is an onset of ESE intensity at  $B_{0\parallel} = hf/g_z\mu_B$ , followed by increasing intensity and eventual divergence at  $B_{0\perp} = hf/g_x\mu_B$ , immediately followed by a cutoff. This explains the shapes of the colored curves in Extended Data Fig. 1a, where the diverging ESE intensity is avoided via inclusion of 5 mT line broadening.

The hyperfine interaction then shifts the overall ESE intensity pattern by an amount that depends on the coupling strength and the nuclear spin projection,  $m_I (= -7/2, -5/2, \dots, +5/2, +7/2)$ . For complex **2**, which possesses a relatively isotropic hyperfine coupling tensor and negligible nuclear quadrupole interaction (NQI), we can approximately generate the full EPR spectrum by summing eight replicas (colored curves in Extended Data Fig. 1a) of the  $g$ -strained spectra discussed above, spacing them according to the experimental peak positions. As can be seen in Extended Data Fig. 1a (top), there is considerable overlap of adjacent hyperfine components, and this is the reason for the apparent intensity staircase at the low field end of the spectrum. The overall agreement between the simulations and the actual spectra in Fig. 3 (main article) is highly satisfactory. The situation for compound **4** is complicated by the significant NQI (see below), which results in an  $m_I$ -dependent renormalization of both  $B_{\parallel}$  and  $B_{\perp}$ , i.e., the widths of the individual  $g$ -strained profiles vary across the spectrum, being narrower at low fields and broader on the high field side of the spectrum. In order to qualitatively reproduce the simulations given in the main article, we picked the values of  $B_{\parallel}$  and  $B_{\perp}$  straight from the simulated Zeeman diagrams in Figs. 2(a) and (b) (main article). Because of the reduced anisotropy (smaller difference between  $g_{xy}$  and  $g_z$ ) and increased hyperfine interaction relative to **2**, there is far less overlap between the eight  $g$ -strained spectra. Nevertheless, this procedure again gives a reasonable reproduction of the

experimental spectra in Fig. 3 (main article), save for a few features that require explicit consideration of the NQI (see below). It should be stressed that the simulations in Extended Data Fig. 1 are no substitute for the actual simulations based on exact diagonalization of the full Hamiltonian matrix [equation (1), main article]. The aim here is simply to provide qualitative insights into the observed spectral splitting patterns.

*Nuclear quadrupole interaction:* As noted above and in the main article, several aspects of the experimental spectra of **4** can only be reproduced in the simulations upon inclusion of a sizeable NQI. The most pronounced feature in the W-band spectrum (Fig. 3, main article) is a sharp upturn in ESE intensity at the low-field edge (at ~2.93 T). Extended Data Fig. 1b shows an expanded view of this part of the spectrum with simulations superimposed for values of  $Q_{zz}$  ranging from 0 to 100 MHz in 25 MHz steps, clearly indicating that a value  $\geq 75$  MHz is needed to reproduce the upturn. The source of this upturn is related to the fact that the NQI introduces an additional source of significant anisotropy to the spin Hamiltonian, resulting in a further redistribution of the ESE intensity as a function of  $\theta$ . The net effect is the recovery of a small divergence (i.e., a peak) in the intensity at the low-field ( $g_z$  or  $\theta = 0$ ) edges of each  $g$ -strained profile (not seen in Extended Data Fig. 1a, which did not explicitly take into account this intensity redistribution). The effect is most pronounced at the low-field edge of the spectrum of compound **4** (at ~2.93 T, see Extended Data Fig. 1b). However, it is also responsible for the small shoulders on the high-field edges of some of the experimental peaks (see Fig. 3, main article), which are not seen for compounds **2** and **3**.

Extended Data Fig. 2 compares X-band simulations both without (a) and with (b,c) an NQI. The formally forbidden (8)  $\rightarrow$  (10) resonance (see Fig. 2c, main article), which is seen very clearly in the experimental spectra (Figs 4 and 5, main article), can only be reproduced in perpendicular mode upon inclusion of an NQI (it does not appear at all in parallel mode), whereupon it becomes weakly allowed. An axial tensor with  $Q_{zz} = 100 \pm 20$  MHz yields the best overall simulations of the combined W- and X-band datasets for **4**. Given that the large quadrupole moment of the  $^{175}\text{Lu}$  nucleus ( $3.49 \text{ b}$ )<sup>20</sup> is one of the main factors behind this magnitude of the NQI, it is natural to consider a similar interaction for compound **3**. In fact, the optimum simulations suggest a somewhat weaker NQI with  $Q_{zz} = 60 \pm 20$  MHz, a trend that is borne out by the computational studies which



predict a weaker electric field gradient (EFG) at the nucleus. The associated  $\pm 20$  MHz uncertainty reflects the fact that it is the relative intensities of spectral peaks that primarily constrain the NQI, rather than the peak positions. Finally, given that the quadrupole moment of the  $^{139}\text{La}$  nucleus is less than 6% that of  $^{175}\text{Lu}$ , we did not include an NQI in the simulations of compound **2**.

As can be seen from the simulations in Extended Data Fig. 2b, the intensities of the perpendicular mode resonances corresponding to transitions (7)  $\rightarrow$  (8) and (8)  $\rightarrow$  (9) [also weakly allowed (8)  $\rightarrow$  (10)] are relatively constant over the 9.11 to 9.5 GHz frequency range. This is as expected because the associated transition frequencies are linear in  $B_0$ , i.e., these are standard perpendicular mode EPR transitions with matrix elements governed by relatively pure quantum states:  $[F, m_F]$  in the case of (7)  $\rightarrow$  (8) and  $[m_s, m_l]$  in the case of (8)  $\rightarrow$  (9). However, this is not the case for the (7)  $\rightarrow$  (9) parallel mode resonances, or the corresponding weakly allowed signals in the perpendicular mode spectra. The experimental X-band spectra in Figs. 4 and 5 (main article) were normalized by the intensity of the highest field (8)  $\rightarrow$  (9) resonance. Consequently, the (7)  $\rightarrow$  (8) and (8)  $\rightarrow$  (10) resonances also exhibit intensities that are frequency independent, as would be expected on the basis of the simulations in Extended Data Fig. 2. By contrast, the (7)  $\rightarrow$  (9) resonances that evolve into clock transitions below  $\sim 9.25$  GHz exhibit a highly non-monotonic intensity variation with frequency, peaking at 9.20 GHz and almost vanishing at 9.5 GHz. As seen in the simulations, these transitions are quite weak in perpendicular mode, whereas they dominate the parallel mode spectra.

*Long delay time ESE intensity profile in the 300 to 410 mT range:* The ESE spectrum in Fig. 5b of the main article, recorded at 9.16 GHz for the longest delay time ( $2\tau = 26 \mu\text{s}$ ), reveals an intensity profile that increases with increasing field, from an onset at 300 mT to a maximum at 410 mT. This profile can again be attributed to the orientational DOS and the variation of the position of the hyperfine clock transition (HCT) with  $\theta$  (see Fig. 4, main article). The  $A$  strain ( $\Delta_A$  in Table 1, main article) required to achieve the best spectral simulations implies that the HCTs (blue dots in Fig. 4, main article) experience a frequency distribution with a full-width-at-half-maximum of 250 MHz. Such strains are not unexpected for a solution sample given that this work demonstrates a significant variation in the hyperfine coupling strength based on the nature of the coordinating ligands. This

strain also implies that 9.16 GHz ESE measurements will access HCTs both at the low end of the range (< 350 mT) and those at the high end (410 mT). The intensity profile will therefore be dominated by the orientational DOS ( $dN/d\theta$ ) and  $d\theta/dg$ , in much the same way as the individual W-band hyperfine peaks seen in Extended Data Fig. 1a and discussed above; both are maximum for the HCTs at 410 mT, i.e., the density of blue dots in Fig. 4a (main article) is highest in this region, which also corresponds to curves with  $\theta$  at or close to  $90^\circ$ . This accounts for the maximum in the ESE intensity at 410 mT for the longest delay.

#### 4. Spin-Lattice Relaxation Time ( $T_1$ ) Measurements

In addition to the phase memory time ( $T_m$ ) measurements reported in the main article, saturation recovery measurements were employed at several of the most intense points in the X-band ESE spectrum of complex **4** (310, 410 and 720 mT at 9.16 GHz) in order to inform upon the spin-lattice relaxation time; time traces and exponential fits are displayed in Extended Data Fig. 3. The first thing to note is that there is no significant variation in  $T_1$  across the spectrum (to within the experimental uncertainty). This is not unexpected, as the HCTs protect only against magnetic noise and do not prevent energy relaxation. The second key point is that the average  $T_1$  value of  $1.45 \pm 0.3$  ms is more than two orders of magnitude longer than the  $T_m$  value ( $12 \pm 1$   $\mu$ s) deduced from the long delay time data in the inset to Fig. 5a (main article). This suggests that there is plenty of room for further optimization of  $T_m$ , up to a  $T_1$  limited value. Indeed, it is likely that the measurements in Fig. 5 (main article) are still influenced by distributions of molecules in the vicinity of the 410 mT HCT, i.e., they do not reflect the maximum possible phase coherence exactly at the HCT. It should also be noted that a  $T_1$  time exceeding 1 ms is also consistent with the weak spin-orbit anisotropy associated with the mixed 5d/6s electronic character of the unpaired spin, which does not impart significant spin-lattice coupling. Therefore, the situation in Lu(II) contrasts that of crystal-field driven clock transitions where much shorter  $T_1$  times have been reported.<sup>21</sup>

#### 5. Computational Details

Each DFT calculation was performed using the resolution-of-the-identity (RI)<sup>22</sup> approximation and D3 dispersion corrections.<sup>23</sup> Solvation effects were modeled using the

Conductor-like Screening Model (COSMO).<sup>24</sup> The employed computational methodology was chosen after an extensive survey of basis sets, relativistic methods, and density functionals, representing a useful compromise between computational cost and accuracy. However, the observed trends in SOMO character (Extended Data Table 1) and isotropic hyperfine coupling constants (Table 1, main article) persist for other GGA/mGGA and hybrid functionals, larger basis sets, and a fully-relativistic x2c treatment.

Starting structures were obtained from crystallographic data, and geometry optimizations in C<sub>1</sub> symmetry were performed using the above methodology to a Cartesian gradient norm of 10<sup>-4</sup> au (au = atomic units). Vibrational analysis was used to confirm that the structures represented minima. Molecular visualizations (Extended Data Fig. 4) were constructed using the Visual Molecular Dynamics software.<sup>25</sup>

*DFT Approach to Hyperfine Coupling Constants:*

$$A_{\text{iso}} = \frac{4\pi}{3} g_e g_n \mu_B \mu_N \langle S_z \rangle^{-1} \int n_s(\mathbf{r}) \rho(\mathbf{r}) d^3\mathbf{r}. \quad (1)$$

The isotropic hyperfine coupling constants for the Ln nuclei in **2**, **3**, and **4** were computed using equation (1), where  $\langle S_z \rangle$  is the expectation value of the spin operator in the z direction, and  $\int n_s(\mathbf{r}) \rho(\mathbf{r}) d^3\mathbf{r}$  is a Fermi contact-like interaction involving the spin density,  $n_s(\mathbf{r})$ , over a nuclear charge distribution  $\rho(\mathbf{r})$ . For the present study, this charge distribution is modeled as both a point charge and as a finite spherical Gaussian charge distribution. The choice of a point charge simply takes  $\rho(\mathbf{r})$  to be a delta function, and the integral thus simplifies to the spin density at the point of the nucleus. For the finite nucleus model, a Gaussian charge distribution was chosen according to the procedure detailed by Malkin et al.<sup>26</sup>

$$\rho(\mathbf{r}) = eZ \left( \frac{\xi}{\pi} \right)^{\frac{3}{2}} e^{-\xi|r-R|^2}, \quad (2)$$

and  $\xi$  is approximated in 1/fm<sup>2</sup> by

$$\xi = 1.5 (0.836M^{1/3} + 0.570)^{-1}, \quad (3)$$

where  $M$  is the mass number,  $Z$  is the nuclear charge,  $\xi$  is the Gaussian coefficient, and  $\mathbf{R}$  is the position of the Ln nucleus. Using this model nuclear charge density, the Fermi integral was evaluated with Gauss-Hermite quadrature. Nuclear  $g$ -factors were taken to be 0.6378 for  $^{175}\text{Lu}$  and 0.7952 for  $^{139}\text{La}$  from Ref. [20].

*Nuclear Quadrupole Interaction:* The EFGs calculated at the position of each Ln nucleus are given in Table 4, and were used to approximate the NQI coupling tensors,  $\vec{Q}$ , using equation (2) in the main article.  $\vec{Q}$  can also be obtained using  $\vec{V}$  in au ( $= E_h/ea_0$ , where  $a_0$  is the Bohr radius) and  $Q$  in barn (b) with the following equation, which includes the necessary conversion factors:

$$\vec{Q}(\text{MHz}) = -5.5944 \times Q(\text{b}) \times \vec{V}(\text{au}). \quad (4)$$

**Table 4:** Calculated EFGs in the molecular frame of reference for compounds **2** – **4** using all-electron, scalar relativistic DFT.

Compound	$V_{xx}$ (au)	$V_{yy}$ (au)	$V_{zz}$ (au)	$V_{xy}$ (au)	$V_{xz}$ (au)	$V_{yz}$ (au)
[Lu(OAr*) <sub>3</sub> ] <sup>-</sup> <b>4</b>	0.392	0.406	-0.797	-0.005	-0.139	0.048
[Lu(N*) <sub>3</sub> ] <sup>-</sup> <b>3</b>	0.286	-0.572	0.286	-0.001	-0.000	-0.001
[La(OAr*) <sub>3</sub> ] <sup>-</sup> <b>2</b>	0.188	0.195	-0.382	-0.003	-0.007	-0.022

Experimental quadrupole moments of 3.49 b and 0.20 b were used for Lu and La nuclei, respectively from Ref [20]. The results are tabulated in Tables 5 and 6. Ellipsoid plots of the nuclear quadrupole moments are visualized in Extended Data Fig. 5 using Jmol.<sup>27</sup> These surface plots are defined by the real space vector,  $\mathbf{r}$ , according to the parametric equation:

$$\mathbf{r}^T \vec{T}^{-1} \mathbf{r} = s^2, \quad (5)$$

where equation (6) gives the nuclear quadrupole moment tensor in the principal axes system,

$$\vec{T} = \frac{Q}{2} \begin{pmatrix} -(1-\eta) & 0 & 0 \\ 0 & -(1+\eta) & 0 \\ 0 & 0 & 2 \end{pmatrix} = \frac{2I(2I-1)h}{eV_{zz}} \vec{Q}, \quad (6)$$

and  $s$  is a dimensionless scale factor.

**Table 5:** Calculated quadrupole coupling tensor in the molecular frame of reference for compounds **2** – **4** using all-electron, scalar relativistic DFT.

Compound	$Q_{xx}$ (MHz)	$Q_{yy}$ (MHz)	$Q_{zz}$ (MHz)	$Q_{xy}$ (MHz)	$Q_{xz}$ (MHz)	$Q_{yz}$ (MHz)
[Lu(OAr*) <sub>3</sub> ] <sup>-</sup> <b>4</b>	-7.64	-7.93	15.6	0.098	2.71	0.938
[Lu(N*) <sub>3</sub> ] <sup>-</sup> <b>3</b>	-5.60	11.2	-5.60	0.020	0	0.019
[La(OAr*) <sub>3</sub> ] <sup>-</sup> <b>2</b>	-0.210	-0.218	0.429	0	0.008	0.025

**Table 6:** Eigenvalues of the quadrupole coupling tensor in the principal axes frame for the three compounds **2** – **4** investigated in this work calculated by DFT.

Compound	$Q_{xx}$ (MHz)	$Q_{yy}$ (MHz)	$Q_{zz}$ (MHz)	$\eta = (Q_{xx} - Q_{yy})/Q_{zz}$
[Lu(OAr*) <sub>3</sub> ] <sup>-</sup> <b>4</b>	-7.76	-8.17	15.9	0.026
[Lu(N*) <sub>3</sub> ] <sup>-</sup> <b>3</b>	-5.57	-5.60	11.2	0.002
[La(OAr*) <sub>3</sub> ] <sup>-</sup> <b>2</b>	-0.194	-0.243	0.436	0.111

## 6. Crystallography

### *X-ray Data Collection, Structure Solution and Refinement for Lu(OAr\*)<sub>3</sub>*

A colorless crystal of approximate dimensions 0.295 × 0.386 × 0.569 mm was mounted in a cryoloop and transferred to a Bruker SMART APEX II diffractometer. The APEX2<sup>28</sup> program package was used to determine the unit-cell parameters and for data collection (120 sec/frame scan time). The raw frame data was processed using SAINT<sup>29</sup> and SADABS<sup>30</sup> to yield the reflection data file. Subsequent calculations were carried out using the SHELXTL<sup>31</sup> program package. The diffraction symmetry was *2/m* and the systematic absences were consistent with the monoclinic space group *P2<sub>1</sub>/n* that was later determined to be correct.

The structure was solved<sup>1</sup> by direct methods and refined on  $F^2$  by full-matrix least-squares techniques (Tables 7 – 10 after References). The analytical scattering factors<sup>32</sup> for neutral atoms were used throughout the analysis. Hydrogen atoms were included using a riding model. There was one molecule of *n*-hexane solvent present. Disordered atoms were included using multiple components with partial site-occupancy-factors.

Least-squares analysis yielded  $wR2 = 0.1086$  and  $Goof = 1.186$  for 912 variables refined against 22343 data ( $0.75 \text{ \AA}$ ),  $R1 = 0.0468$  for those 19679 data with  $I > 2.0\sigma(I)$ . There were several high residuals present in the final difference-Fourier map. It was not possible to determine the nature of the residuals although it was probable that additional *n*-hexane solvent was present. The SQUEEZE<sup>33</sup> routine in the PLATON<sup>34</sup> program package was used to account for the electrons in the solvent accessible voids.

#### *X-ray Data Collection, Structure Solution and Refinement for [K(crypt)][Lu(OAr\*)<sub>3</sub>].3Et<sub>2</sub>O*

A purple crystal of approximate dimensions  $0.198 \times 0.267 \times 0.274 \text{ mm}$  was mounted in a cryoloop and transferred to a Bruker SMART APEX II diffractometer. The APEX2<sup>28</sup> program package was used to determine the unit-cell parameters and for data collection (120 sec/frame scan time). The raw frame data was processed using SAINT<sup>29</sup> and SADABS<sup>30</sup> to yield the reflection data file. Subsequent calculations were carried out using the SHELXTL<sup>31</sup> program package. There were no systematic absences nor any diffraction symmetry other than the Friedel condition. The centrosymmetric triclinic space group  $P\bar{1}$  was assigned and later determined to be correct.

The structure was solved<sup>1</sup> by direct methods and refined on  $F^2$  by full-matrix least-squares techniques (Tables 11 – 14 after References). The analytical scattering factors<sup>32</sup> for neutral atoms were used throughout the analysis. Hydrogen atoms were included using a riding model. There were three molecules of diethylether solvent present. Least-squares analysis yielded  $wR2 = 0.1183$  and  $Goof = 1.055$  for 1240 variables refined against 27368 data ( $0.75 \text{ \AA}$ ),  $R1 = 0.0465$  for those 22821 data with  $I > 2.0\sigma(I)$ .

## 7. References

- <sup>1</sup> CCDC 2074946 ([K(crypt)][Lu(OAr\*)<sub>3</sub>]) and 2074947 (Lu(OAr\*)<sub>3</sub>) contain supplementary crystallographic data for this paper, which can be obtained free of charge via [www.ccdc.cam.ac.uk/data\\_request/cif](http://www.ccdc.cam.ac.uk/data_request/cif), by emailing [data\\_request@ccdc.cam.ac.uk](mailto:data_request@ccdc.cam.ac.uk), or by contacting The Cambridge Crystallographic Data Centre, 12 Union Road, Cambridge CB2 1EZ, UK; fax: +44 1223 336033.
- <sup>2</sup> Moehring, S. A. *et al.* Room-Temperature Stable Y(II) Aryloxide: Using Steric Saturation to Kinetically Stabilize Y(II) Complexes. *Inorg. Chem.* **59**, 3207-3214 (2020). <https://doi.org/10.1021/acs.inorgchem.9b03587>

- <sup>3</sup> MacDonald, M. R., Bates, J. E., Ziller, J. W., Furche, F., Evans, W. J. Completing the Series of +2 Ions for the Lanthanide Elements: Synthesis of Molecular Complexes of Pr<sup>2+</sup>, Gd<sup>2+</sup>, Tb<sup>2+</sup>, and Lu<sup>2+</sup>. *J. Am. Chem. Soc.* **135**, 9857-9868 (2013). <https://doi.org/10.1021/ja403753j>
- <sup>4</sup> Guzei, I. A., Wendt, M. An improved method for the computation of ligand steric effects based on solid angles. *Dalton Trans.* 2006, 3991-3999. <https://doi.org/10.1039/B605102B>
- <sup>5</sup> Evans, W. J. Tutorial on the role of cyclopentadienyl ligands in the discovery of molecular complexes of the rare-earth and actinide metals in new oxidation states. *Organometallics* **35**, 3088-3100 (2016). <https://doi.org/10.1021/acs.organomet.6b00466>
- <sup>6</sup> Moehring, S. A. et al., Rare-Earth Metal(II) Aryloxides: Structure, Synthesis, and EPR Spectroscopy of [K(2.2.2-cryptand)][Sc(OC<sub>6</sub>H<sub>2</sub>tBu<sub>2</sub>-2,6-Me-4)<sub>3</sub>]. *Chem. - A Eur. J.* **24**, 18059-18067 (2018). <https://doi.org/10.1002/chem.201803807>
- <sup>7</sup> Peterson, J. K., MacDonald, M. R., Ziller, J. W., Evans, W. J. Synthetic Aspects of (C<sub>5</sub>H<sub>4</sub>SiMe<sub>3</sub>)<sub>3</sub>Ln Rare-Earth Chemistry: Formation of (C<sub>5</sub>H<sub>4</sub>SiMe<sub>3</sub>)<sub>3</sub>Lu via [(C<sub>5</sub>H<sub>4</sub>SiMe<sub>3</sub>)<sub>2</sub>Ln]<sup>+</sup> Metallocene Precursors. *Organometallics* **32**, 2625-2631 (2013). <https://doi.org/10.1021/om400116d>
- <sup>8</sup> Evans, W. J., Lee, D. S., Johnston, M. A., Ziller, J. W. The Elusive (C<sub>5</sub>Me<sub>4</sub>H)<sub>3</sub>Lu: Its Synthesis and LnZ<sub>3</sub>/K/N<sub>2</sub> Reactivity. *Organometallics* **24**, 6393-6397 (2005). <https://doi.org/10.1021/om050709k>
- <sup>9</sup> Scarel, G., et al., [(Me<sub>3</sub>Si)<sub>2</sub>N]<sub>3</sub>Lu: Molecular Structure and Use as Lu and Si Source for Atomic Layer Deposition of Lu Silicate Films. *Z. Anorg. Allg. Chem.* **633**, 2097-2103 (2007). <https://doi.org/10.1002/zaac.200700223>
- <sup>10</sup> Steele, L. A. M., Boyle, T. J., Kemp, R. A., Moore, C. The selective insertion of carbon dioxide into a lanthanide(III) 2,6-di-*t*-butyl-phenoxide bond. *Polyhedron* **42**, 258-264 (2012). <https://doi.org/10.1016/j.poly.2012.05.021>
- <sup>11</sup> Ryan, A. J., Ziller, J. W., Evans, W. J. The importance of the counter-cation in reductive rare-earth metal chemistry: 18-crown-6 instead of 2,2,2-cryptand allows isolation of [Y<sup>II</sup>(NR<sub>2</sub>)<sub>3</sub>]<sup>1-</sup> and ynediolate and enediolate complexes from CO reactions. *Chem. Sci.* **11**, 2006-2014 (2020). <https://doi.org/10.1039/C9SC05794C>
- <sup>12</sup> Edelmann, F. T. *Synthetic Methods of Organometallic and Inorganic Chemistry, Volume 6: Lanthanides and Actinides*; Herrmann, W. A., Ed.; 1996.
- <sup>13</sup> Watanabe, T., Ishida, Y., Matsuo, T., Kawaguchi, H. Syntheses and structures of zirconium(IV) complexes supported by 2,6-di-adamantylaryloxy ligands and formation of arene-bridged dizirconium complexes with an inverse sandwich structure. *Dalton Trans.* **39**, 484-491 (2010). <https://doi.org/10.1039/B911082H>

- <sup>14</sup> Jenkins, T. F. *et al.*, Tetramethylcyclopentadienyl Ligands Allow Isolation of Ln(II) Ions across the Lanthanide Series in [K(2.2.2-cryptand)][(C<sub>5</sub>Me<sub>4</sub>H)<sub>3</sub>Ln] Complexes. *Organometallics* **37**, 3863-3873 (2018). <https://doi.org/10.1021/acs.organomet.8b00557>
- <sup>15</sup> Goodwin, C. A. P. *et al.*, Physicochemical Properties of Near-Linear Lanthanide(II) Bis(silylamide) Complexes (Ln = Sm, Eu, Tm, Yb). *Inorg. Chem.* **55**, 10057-10067 (2016). <https://doi.org/10.1021/acs.inorgchem.6b00808>
- <sup>16</sup> Hitchcock, P. B., Lappert, M. F., Maron, L., Protchenko, A. V. Lanthanum does form stable molecular compounds in the +2 oxidation state. *Angew. Chem. Int. Ed.* **47**, 1488-1491 (2008). <https://doi.org/10.1002/anie.200704887>
- <sup>17</sup> Goodwin, C. A. P., Reta, D., Ortu, F., Chilton, N. F., Mills, D. P. Synthesis and Electronic Structures of Heavy Lanthanide Metallocenium Cations. *J. Am. Chem. Soc.* **139**, 18714-18724 (2017). <https://doi.org/10.1021/jacs.7b11535>
- <sup>18</sup> Goodwin, C. A. P. *et al.*, Homoleptic Trigonal Planar Lanthanide Complexes Stabilized by Superbulky Silylamide Ligands. *Organometallics* **34**, 2314-2325 (2015). <https://doi.org/10.1021/om501123e>
- <sup>19</sup> Huh, D. N., Roy, S., Ziller, J. W., Furche, F., Evans, W. J. Isolation of a Square-Planar Th(III) Complex: Synthesis and Structure of [Th(OC<sub>6</sub>H<sub>2</sub>Bu<sub>2</sub>-2,6-Me-4)<sub>4</sub>]<sup>1-</sup>. *J. Am. Chem. Soc.* **141**, 12458-12463. <https://doi.org/10.1021/jacs.9b04399>
- <sup>20</sup> Stone, N. J. Table of nuclear electric quadrupole moments. *Atomic Data and Nuclear Data Tables* **111-112**, 1-28 (2016). <https://doi.org/10.1016/j.adt.2015.12.002>
- <sup>21</sup> Shiddiq, M. *et al.* Enhancing coherence in molecular spin qubits via atomic clock transitions, *Nature* **531**, 348-351 (2016). <https://doi.org/10.1038/nature16984>
- <sup>22</sup> Neese, F., Olbrich, G. Efficient use of the resolution of the identity approximation in time-dependent density functional calculations with hybrid density functionals. *Chem. Phys. Lett.* **362**, 170-178 (2002). [https://doi.org/10.1016/S0009-2614\(02\)01053-9](https://doi.org/10.1016/S0009-2614(02)01053-9)
- <sup>23</sup> Grimme, S., Antony, J., Ehrlich, S., Krieg, H. J. A consistent and accurate *ab initio* parametrization of density functional dispersion correction (DFT-D) for the 94 elements H-Pu. *Chem. Phys.* **132**, 154104 (2010). <https://doi.org/10.1063/1.3382344>
- <sup>24</sup> Klamt, A., Schüürmann, G. COSMO: a new approach to dielectric screening in solvents with explicit expressions for the screening energy and its gradient. *J. Chem. Soc., Perkin Trans. 2* **1993**, 799-805. <https://doi.org/10.1039/P29930000799>
- <sup>25</sup> Humphrey, W., Dalke, A., Schulten, K. J. VMD: Visual molecular dynamics. *Molec. Graphics* **14**, 33-38 (1996). [https://doi.org/10.1016/0263-7855\(96\)00018-5](https://doi.org/10.1016/0263-7855(96)00018-5)



- <sup>26</sup> Malkin, E., Malkin, I., Malkina, O. L., Malkin, V. G., Kaupp, M. Scalar relativistic calculations of hyperfine coupling tensors using the Douglas–Kroll–Hess method with a finite-size nucleus model. *Phys. Chem. Chem. Phys.* **8**, 4079-4085 (2006). <https://doi.org/10.1039/B607044B>
- <sup>27</sup> Hanson, R. M. Jmol – a paradigm shift in crystallographic visualization. *J. Appl. Cryst.* **43**, 1250-1260 (2010). <https://doi.org/10.1107/S0021889810030256>
- <sup>28</sup> APEX2; Version 2014.11-0; Bruker AXS, Inc.: Madison, WI, 2014.
- <sup>29</sup> SAINT; Version 8.34a; Bruker AXS, Inc.: Madison, WI, 2013.
- <sup>30</sup> Sheldrick, G. M. SADABS; Version 2014/5; Bruker AXS, Inc.: Madison, WI, 2014.
- <sup>31</sup> Sheldrick, G. M. SHELXTL; Version 2014/7; Bruker AXS, Inc.: Madison, WI, 2014.
- <sup>32</sup> *International Tables for Crystallography*, Vol. C.; Dordrecht: Kluwer Academic Publishers., 1992.
- <sup>33</sup> Spek, A. L. PLATON SQUEEZE: a tool for the calculation of the disordered solvent contribution to the calculated structure factors. *Acta Crystallogr. Sect. C Struct. Chem.* **71**, 9-18 (2015). <https://doi.org/10.1107/S2053229614024929>
- <sup>34</sup> Spek, A. L. Structure validation in chemical crystallography. *Acta Crystallogr. Sect. D* **65**, 148-155 (2009). <https://doi.org/10.1107/S090744490804362X>

**Table 7:** Atomic coordinates ( $\times 10^4$ ) and equivalent isotropic displacement parameters ( $\text{\AA}^2 \times 10^3$ ) for  $\text{Lu}(\text{OAr}^*)_3$ .  $U(\text{eq})$  is defined as one third of the trace of the orthogonalized  $U^{ij}$  tensor.

	x	y	z	$U(\text{eq})$
Lu(1)	2610(1)	7186(1)	6733(1)	13(1)
O(1)	1485(2)	6953(1)	6005(1)	17(1)
O(2)	3460(2)	7540(1)	6355(1)	16(1)
O(3)	3316(2)	6761(1)	7448(1)	16(1)
C(1)	575(2)	6803(1)	5786(2)	14(1)
C(2)	-177(2)	7135(1)	5585(2)	15(1)
C(3)	-1120(2)	6982(1)	5431(2)	16(1)
C(4)	-1355(2)	6520(1)	5446(2)	19(1)
C(5)	-612(2)	6209(1)	5604(2)	19(1)
C(6)	357(2)	6332(1)	5765(2)	15(1)
C(7)	36(2)	7646(1)	5524(2)	15(1)
C(8)	642(2)	7714(1)	5073(2)	16(1)
C(9)	870(2)	8221(1)	5018(2)	19(1)
C(10)	1421(2)	8413(1)	5685(2)	21(1)
C(11)	794(2)	8369(1)	6123(2)	19(1)
C(12)	-144(2)	8637(1)	5830(2)	21(1)
C(13)	-682(2)	8436(1)	5169(2)	20(1)
C(14)	-893(2)	7929(1)	5236(2)	17(1)
C(15)	550(2)	7868(1)	6185(2)	15(1)
C(16)	-64(3)	8491(1)	4729(2)	23(1)
C(17)	-2414(3)	6382(1)	5289(2)	26(1)
C(18)	-2790(3)	6562(2)	5811(2)	39(1)
C(19)	-3030(3)	6593(2)	4642(2)	43(1)
C(20)	-2548(3)	5865(2)	5237(4)	74(2)
C(21)	1080(2)	5931(1)	5885(2)	16(1)
C(22)	2150(2)	6058(1)	6038(2)	24(1)
C(23)	2781(3)	5625(1)	6106(2)	32(1)
C(24)	2691(3)	5338(1)	6660(2)	41(1)
C(25)	1642(3)	5197(1)	6518(2)	30(1)
C(26)	1305(3)	4920(1)	5902(2)	26(1)
C(27)	1417(3)	5204(1)	5347(2)	23(1)
C(28)	807(2)	5640(1)	5267(2)	18(1)
C(29)	1016(3)	5628(1)	6444(2)	26(1)
C(30)	2465(3)	5347(1)	5489(2)	32(1)
C(31)	4292(2)	7746(1)	6381(2)	14(1)
C(32)	4753(2)	8047(1)	6888(2)	15(1)
C(33)	5638(2)	8230(1)	6894(2)	19(1)
C(34)	6070(2)	8129(1)	6441(2)	19(1)
C(35)	5583(2)	7836(1)	5942(2)	17(1)
C(36)	4695(2)	7646(1)	5889(2)	14(1)
C(37)	4373(2)	8216(1)	7425(2)	15(1)
C(38)	5124(2)	8116(1)	8095(2)	20(1)
C(39)	4815(2)	8318(1)	8639(2)	23(1)
C(40)	4689(3)	8835(1)	8552(2)	27(1)

C(41)	3920(3)	8938(1)	7910(2)	23(1)
C(42)	2966(3)	8727(1)	7907(2)	23(1)
C(43)	3099(2)	8210(1)	7995(2)	20(1)
C(44)	3420(2)	8002(1)	7453(2)	17(1)
C(45)	4211(3)	8739(1)	7356(2)	21(1)
C(46)	3863(3)	8102(1)	8642(2)	23(1)
C(47)	7065(2)	8315(1)	6479(2)	24(1)
C(48)	7792(3)	7927(2)	6671(2)	38(1)
C(49)	7044(3)	8504(2)	5826(2)	34(1)
C(50)	7393(3)	8701(2)	6971(2)	42(1)
C(51)	4161(2)	7343(1)	5311(2)	14(1)
C(52)	3176(2)	7559(1)	4943(2)	17(1)
C(53)	2618(2)	7258(1)	4372(2)	20(1)
C(54)	3184(2)	7219(1)	3880(2)	26(1)
C(55)	4160(3)	7003(1)	4245(2)	24(1)
C(56)	4012(3)	6525(1)	4471(2)	24(1)
C(57)	3454(2)	6557(1)	4947(2)	20(1)
C(58)	4019(2)	6851(1)	5519(2)	17(1)
C(59)	4717(2)	7300(1)	4825(2)	19(1)
C(60)	2476(2)	6781(1)	4613(2)	20(1)
C(61)	3356(2)	6394(1)	7831(2)	17(1)
C(62)	2574(2)	6277(1)	8035(2)	19(1)
C(63)	2601(3)	5851(1)	8329(2)	28(1)
C(64)	3365(3)	5552(1)	8451(2)	32(1)
C(65)	4171(3)	5706(1)	8319(2)	24(1)
C(66)	4204(2)	6120(1)	8017(2)	17(1)
C(67)	1733(2)	6597(1)	8049(2)	19(1)
C(68)	1607(2)	7048(1)	7662(2)	20(1)
C(69)	816(3)	7351(1)	7762(2)	27(1)
C(70)	-140(3)	7098(2)	7532(2)	34(1)
C(71)	-54(3)	6655(2)	7909(2)	30(1)
C(72)	188(3)	6763(2)	8628(2)	33(1)
C(73)	1138(3)	7025(2)	8854(2)	29(1)
C(74)	1939(3)	6730(1)	8763(2)	24(1)
C(75)	743(3)	6355(1)	7804(2)	28(1)
C(76)	1063(3)	7467(2)	8471(2)	30(1)
C(77)	3342(3)	5073(2)	8734(3)	54(2)
C(78)	3636(5)	4706(2)	8259(3)	39(2)
C(79)	4044(5)	5020(2)	9362(3)	44(2)
C(80)	2327(4)	4906(2)	8632(4)	44(2)
C(78B)	3100(9)	5186(4)	9406(5)	44(4)
C(79B)	4358(7)	4878(4)	9056(6)	29(3)
C(80B)	2572(11)	4768(5)	8352(8)	63(6)
C(81)	5127(2)	6268(1)	7880(2)	17(1)
C(82)	5415(2)	6765(1)	8100(2)	19(1)
C(83)	6327(2)	6908(1)	7955(2)	24(1)
C(84)	6162(3)	6864(1)	7234(2)	27(1)
C(85)	5920(3)	6370(1)	7025(2)	25(1)
C(86)	6756(3)	6060(1)	7393(2)	27(1)
C(87)	6910(2)	6106(1)	8113(2)	25(1)
C(88)	5989(2)	5958(1)	8244(2)	24(1)
C(89)	5006(2)	6223(1)	7163(2)	21(1)
C(90)	7165(2)	6598(1)	8324(2)	26(1)

C(91)	4709(6)	3677(3)	7208(4)	87(1)
C(92)	4850(6)	4180(3)	7176(4)	87(1)
C(93)	4966(6)	4338(3)	6571(4)	87(1)
C(94)	5200(6)	4834(3)	6515(4)	87(1)
C(95)	5154(6)	4966(3)	5836(4)	87(1)
C(96)	5303(6)	5462(3)	5725(4)	87(1)

---

**Table 8:** Bond lengths [Å] and angles [°] for Lu(OAr\*)<sub>3</sub>.

---

Lu(1)-O(2)	2.002(2)
Lu(1)-O(3)	2.014(2)
Lu(1)-O(1)	2.020(2)
O(1)-C(1)	1.344(4)
O(2)-C(31)	1.350(4)
O(3)-C(61)	1.355(4)
C(1)-C(6)	1.410(5)
C(1)-C(2)	1.433(4)
C(2)-C(3)	1.394(4)
C(2)-C(7)	1.541(5)
C(3)-C(4)	1.398(5)
C(4)-C(5)	1.379(5)
C(4)-C(17)	1.538(5)
C(5)-C(6)	1.404(4)
C(6)-C(21)	1.550(5)
C(7)-C(14)	1.550(4)
C(7)-C(8)	1.550(4)
C(7)-C(15)	1.551(4)
C(8)-C(9)	1.532(5)
C(9)-C(16)	1.537(5)
C(9)-C(10)	1.539(5)
C(10)-C(11)	1.543(5)
C(11)-C(15)	1.525(5)
C(11)-C(12)	1.540(5)
C(12)-C(13)	1.534(5)
C(13)-C(14)	1.533(5)
C(13)-C(16)	1.538(5)
C(17)-C(18)	1.522(6)
C(17)-C(20)	1.525(6)
C(17)-C(19)	1.550(6)
C(21)-C(29)	1.545(5)
C(21)-C(28)	1.547(5)
C(21)-C(22)	1.548(5)
C(22)-C(23)	1.552(5)
C(23)-C(30)	1.521(6)
C(23)-C(24)	1.523(7)
C(24)-C(25)	1.533(6)
C(25)-C(26)	1.521(5)
C(25)-C(29)	1.541(6)
C(26)-C(27)	1.530(5)
C(27)-C(30)	1.533(5)
C(27)-C(28)	1.539(5)
C(31)-C(32)	1.414(4)
C(31)-C(36)	1.426(4)
C(32)-C(33)	1.405(5)
C(32)-C(37)	1.546(4)
C(33)-C(34)	1.380(5)
C(34)-C(35)	1.396(5)
C(34)-C(47)	1.542(5)
C(35)-C(36)	1.392(4)

C(36)-C(51)	1.542(4)
C(37)-C(45)	1.548(5)
C(37)-C(44)	1.558(5)
C(37)-C(38)	1.563(4)
C(38)-C(39)	1.532(5)
C(39)-C(40)	1.528(6)
C(39)-C(46)	1.540(5)
C(40)-C(41)	1.531(5)
C(41)-C(42)	1.535(5)
C(41)-C(45)	1.536(5)
C(42)-C(43)	1.529(5)
C(43)-C(46)	1.540(5)
C(43)-C(44)	1.545(4)
C(47)-C(48)	1.525(6)
C(47)-C(50)	1.532(6)
C(47)-C(49)	1.533(6)
C(51)-C(58)	1.544(5)
C(51)-C(52)	1.551(4)
C(51)-C(59)	1.551(4)
C(52)-C(53)	1.540(5)
C(53)-C(60)	1.530(5)
C(53)-C(54)	1.572(5)
C(54)-C(55)	1.539(5)
C(55)-C(56)	1.525(6)
C(55)-C(59)	1.543(5)
C(56)-C(57)	1.532(5)
C(57)-C(58)	1.532(5)
C(57)-C(60)	1.538(5)
C(61)-C(62)	1.409(5)
C(61)-C(66)	1.428(5)
C(62)-C(63)	1.399(5)
C(62)-C(67)	1.561(5)
C(63)-C(64)	1.381(5)
C(64)-C(65)	1.387(5)
C(64)-C(77)	1.538(5)
C(65)-C(66)	1.390(5)
C(66)-C(81)	1.547(5)
C(67)-C(68)	1.548(5)
C(67)-C(74)	1.554(5)
C(67)-C(75)	1.555(5)
C(68)-C(69)	1.537(5)
C(69)-C(76)	1.523(5)
C(69)-C(70)	1.526(6)
C(70)-C(71)	1.525(6)
C(71)-C(72)	1.541(6)
C(71)-C(75)	1.541(5)
C(72)-C(73)	1.532(6)
C(73)-C(74)	1.526(5)
C(73)-C(76)	1.527(6)
C(77)-C(79)	1.444(6)
C(77)-C(80B)	1.476(8)
C(77)-C(80)	1.521(6)
C(77)-C(79B)	1.544(8)

C(77)-C(78)	1.653(7)
C(77)-C(78B)	1.665(8)
C(81)-C(89)	1.538(5)
C(81)-C(82)	1.548(5)
C(81)-C(88)	1.555(5)
C(82)-C(83)	1.537(5)
C(83)-C(84)	1.535(6)
C(83)-C(90)	1.536(5)
C(84)-C(85)	1.526(6)
C(85)-C(86)	1.533(5)
C(85)-C(89)	1.536(5)
C(86)-C(87)	1.535(5)
C(87)-C(90)	1.520(6)
C(87)-C(88)	1.539(5)
C(91)-C(92)	1.489(10)
C(92)-C(93)	1.474(11)
C(93)-C(94)	1.505(10)
C(94)-C(95)	1.527(11)
C(95)-C(96)	1.497(10)

O(2)-Lu(1)-O(3)	114.24(9)
O(2)-Lu(1)-O(1)	107.94(9)
O(3)-Lu(1)-O(1)	119.84(9)
C(1)-O(1)-Lu(1)	149.8(2)
C(31)-O(2)-Lu(1)	153.4(2)
C(61)-O(3)-Lu(1)	152.2(2)
O(1)-C(1)-C(6)	121.3(3)
O(1)-C(1)-C(2)	118.3(3)
C(6)-C(1)-C(2)	120.4(3)
C(3)-C(2)-C(1)	117.9(3)
C(3)-C(2)-C(7)	120.4(3)
C(1)-C(2)-C(7)	121.6(3)
C(2)-C(3)-C(4)	122.8(3)
C(5)-C(4)-C(3)	117.3(3)
C(5)-C(4)-C(17)	123.4(3)
C(3)-C(4)-C(17)	119.2(3)
C(4)-C(5)-C(6)	123.7(3)
C(5)-C(6)-C(1)	117.6(3)
C(5)-C(6)-C(21)	115.8(3)
C(1)-C(6)-C(21)	126.6(3)
C(2)-C(7)-C(14)	112.0(3)
C(2)-C(7)-C(8)	110.9(3)
C(14)-C(7)-C(8)	106.5(3)
C(2)-C(7)-C(15)	112.0(3)
C(14)-C(7)-C(15)	105.1(3)
C(8)-C(7)-C(15)	109.9(3)
C(9)-C(8)-C(7)	111.3(3)
C(8)-C(9)-C(16)	109.9(3)
C(8)-C(9)-C(10)	109.8(3)
C(16)-C(9)-C(10)	109.5(3)
C(9)-C(10)-C(11)	109.3(3)
C(15)-C(11)-C(12)	108.7(3)
C(15)-C(11)-C(10)	110.0(3)

C(12)-C(11)-C(10)	109.5(3)
C(13)-C(12)-C(11)	108.8(3)
C(14)-C(13)-C(12)	109.7(3)
C(14)-C(13)-C(16)	110.0(3)
C(12)-C(13)-C(16)	109.3(3)
C(13)-C(14)-C(7)	112.1(3)
C(11)-C(15)-C(7)	112.1(3)
C(9)-C(16)-C(13)	108.6(3)
C(18)-C(17)-C(20)	109.1(4)
C(18)-C(17)-C(4)	109.3(3)
C(20)-C(17)-C(4)	111.9(3)
C(18)-C(17)-C(19)	108.1(3)
C(20)-C(17)-C(19)	107.6(4)
C(4)-C(17)-C(19)	110.7(3)
C(29)-C(21)-C(28)	108.9(3)
C(29)-C(21)-C(22)	106.6(3)
C(28)-C(21)-C(22)	106.3(3)
C(29)-C(21)-C(6)	110.7(3)
C(28)-C(21)-C(6)	107.2(3)
C(22)-C(21)-C(6)	116.8(3)
C(21)-C(22)-C(23)	111.2(3)
C(30)-C(23)-C(24)	110.1(3)
C(30)-C(23)-C(22)	110.3(3)
C(24)-C(23)-C(22)	108.8(4)
C(23)-C(24)-C(25)	109.2(3)
C(26)-C(25)-C(24)	110.1(4)
C(26)-C(25)-C(29)	109.2(3)
C(24)-C(25)-C(29)	109.3(3)
C(25)-C(26)-C(27)	109.8(3)
C(26)-C(27)-C(30)	110.3(3)
C(26)-C(27)-C(28)	109.4(3)
C(30)-C(27)-C(28)	108.0(3)
C(27)-C(28)-C(21)	112.2(3)
C(25)-C(29)-C(21)	111.4(3)
C(23)-C(30)-C(27)	109.1(3)
O(2)-C(31)-C(32)	120.6(3)
O(2)-C(31)-C(36)	118.2(3)
C(32)-C(31)-C(36)	121.1(3)
C(33)-C(32)-C(31)	116.9(3)
C(33)-C(32)-C(37)	115.9(3)
C(31)-C(32)-C(37)	127.1(3)
C(34)-C(33)-C(32)	123.8(3)
C(33)-C(34)-C(35)	117.5(3)
C(33)-C(34)-C(47)	122.6(3)
C(35)-C(34)-C(47)	119.9(3)
C(36)-C(35)-C(34)	122.8(3)
C(35)-C(36)-C(31)	117.8(3)
C(35)-C(36)-C(51)	121.0(3)
C(31)-C(36)-C(51)	121.3(3)
C(32)-C(37)-C(45)	108.8(3)
C(32)-C(37)-C(44)	117.2(3)
C(45)-C(37)-C(44)	106.8(3)
C(32)-C(37)-C(38)	110.1(3)



C(45)-C(37)-C(38)	108.6(3)
C(44)-C(37)-C(38)	105.1(3)
C(39)-C(38)-C(37)	111.7(3)
C(40)-C(39)-C(38)	109.7(3)
C(40)-C(39)-C(46)	109.4(3)
C(38)-C(39)-C(46)	110.3(3)
C(39)-C(40)-C(41)	109.7(3)
C(40)-C(41)-C(42)	109.2(3)
C(40)-C(41)-C(45)	110.3(3)
C(42)-C(41)-C(45)	109.6(3)
C(43)-C(42)-C(41)	108.5(3)
C(42)-C(43)-C(46)	110.3(3)
C(42)-C(43)-C(44)	110.5(3)
C(46)-C(43)-C(44)	108.8(3)
C(43)-C(44)-C(37)	112.2(3)
C(43)-C(44)-Lu(1)	124.9(2)
C(37)-C(44)-Lu(1)	121.8(2)
C(41)-C(45)-C(37)	111.7(3)
C(43)-C(46)-C(39)	107.9(3)
C(48)-C(47)-C(50)	108.6(4)
C(48)-C(47)-C(49)	109.2(3)
C(50)-C(47)-C(49)	107.8(4)
C(48)-C(47)-C(34)	108.9(3)
C(50)-C(47)-C(34)	112.1(3)
C(49)-C(47)-C(34)	110.2(3)
C(36)-C(51)-C(58)	111.8(3)
C(36)-C(51)-C(52)	109.9(3)
C(58)-C(51)-C(52)	109.9(3)
C(36)-C(51)-C(59)	112.1(3)
C(58)-C(51)-C(59)	106.3(3)
C(52)-C(51)-C(59)	106.6(3)
C(53)-C(52)-C(51)	111.0(3)
C(60)-C(53)-C(52)	109.5(3)
C(60)-C(53)-C(54)	109.6(3)
C(52)-C(53)-C(54)	110.0(3)
C(55)-C(54)-C(53)	106.5(3)
C(56)-C(55)-C(54)	109.8(3)
C(56)-C(55)-C(59)	109.8(3)
C(54)-C(55)-C(59)	111.2(3)
C(55)-C(56)-C(57)	109.4(3)
C(56)-C(57)-C(58)	109.2(3)
C(56)-C(57)-C(60)	109.0(3)
C(58)-C(57)-C(60)	109.4(3)
C(57)-C(58)-C(51)	111.7(3)
C(55)-C(59)-C(51)	111.2(3)
C(53)-C(60)-C(57)	110.0(3)
O(3)-C(61)-C(62)	120.9(3)
O(3)-C(61)-C(66)	118.8(3)
C(62)-C(61)-C(66)	120.3(3)
C(63)-C(62)-C(61)	117.4(3)
C(63)-C(62)-C(67)	115.4(3)
C(61)-C(62)-C(67)	126.7(3)
C(64)-C(63)-C(62)	123.6(3)

C(63)-C(64)-C(65)	117.0(3)
C(63)-C(64)-C(77)	122.1(3)
C(65)-C(64)-C(77)	120.8(3)
C(64)-C(65)-C(66)	123.2(3)
C(65)-C(66)-C(61)	117.6(3)
C(65)-C(66)-C(81)	120.3(3)
C(61)-C(66)-C(81)	122.1(3)
C(68)-C(67)-C(74)	107.1(3)
C(68)-C(67)-C(75)	105.3(3)
C(74)-C(67)-C(75)	108.7(3)
C(68)-C(67)-C(62)	117.0(3)
C(74)-C(67)-C(62)	105.9(3)
C(75)-C(67)-C(62)	112.5(3)
C(69)-C(68)-C(67)	112.0(3)
C(69)-C(68)-Lu(1)	127.0(2)
C(67)-C(68)-Lu(1)	120.5(2)
C(76)-C(69)-C(70)	109.8(3)
C(76)-C(69)-C(68)	109.5(3)
C(70)-C(69)-C(68)	109.6(3)
C(71)-C(70)-C(69)	109.0(3)
C(70)-C(71)-C(72)	109.7(4)
C(70)-C(71)-C(75)	109.5(3)
C(72)-C(71)-C(75)	109.7(3)
C(73)-C(72)-C(71)	108.7(3)
C(74)-C(73)-C(76)	109.1(3)
C(74)-C(73)-C(72)	109.9(4)
C(76)-C(73)-C(72)	110.3(3)
C(73)-C(74)-C(67)	111.6(3)
C(71)-C(75)-C(67)	111.4(3)
C(69)-C(76)-C(73)	109.3(3)
C(79)-C(77)-C(80)	118.3(5)
C(79)-C(77)-C(64)	112.6(4)
C(80B)-C(77)-C(64)	115.6(7)
C(80)-C(77)-C(64)	112.4(4)
C(80B)-C(77)-C(79B)	119.5(9)
C(64)-C(77)-C(79B)	112.2(5)
C(79)-C(77)-C(78)	106.5(5)
C(80)-C(77)-C(78)	98.3(5)
C(64)-C(77)-C(78)	106.9(4)
C(80B)-C(77)-C(78B)	106.3(8)
C(64)-C(77)-C(78B)	102.7(5)
C(79B)-C(77)-C(78B)	96.8(6)
C(89)-C(81)-C(66)	111.0(3)
C(89)-C(81)-C(82)	109.3(3)
C(66)-C(81)-C(82)	111.8(3)
C(89)-C(81)-C(88)	106.6(3)
C(66)-C(81)-C(88)	111.2(3)
C(82)-C(81)-C(88)	106.7(3)
C(83)-C(82)-C(81)	111.1(3)
C(84)-C(83)-C(90)	109.4(3)
C(84)-C(83)-C(82)	109.7(3)
C(90)-C(83)-C(82)	109.7(3)
C(85)-C(84)-C(83)	109.6(3)

C(84)-C(85)-C(86)	109.2(3)
C(84)-C(85)-C(89)	109.8(3)
C(86)-C(85)-C(89)	109.7(3)
C(85)-C(86)-C(87)	108.8(3)
C(90)-C(87)-C(86)	109.8(3)
C(90)-C(87)-C(88)	110.7(3)
C(86)-C(87)-C(88)	109.0(3)
C(87)-C(88)-C(81)	111.3(3)
C(85)-C(89)-C(81)	111.3(3)
C(87)-C(90)-C(83)	108.5(3)
C(93)-C(92)-C(91)	114.3(7)
C(92)-C(93)-C(94)	118.3(7)
C(93)-C(94)-C(95)	112.6(7)
C(96)-C(95)-C(94)	116.2(7)

---

**Table 9:** Anisotropic displacement parameters ( $\text{\AA}^2 \times 10^3$ ) for  $\text{Lu}(\text{OAr}^*)_3$ . The anisotropic displacement factor exponent takes the form:  $-2\pi^2 [h^2 a^{*2}U^{11} + \dots + 2 h k a^* b^* U^{12}]$ .

	$U^{11}$	$U^{22}$	$U^{33}$	$U^{23}$	$U^{13}$	$U^{12}$
Lu(1)	9(1)	17(1)	11(1)	-1(1)	1(1)	-1(1)
O(1)	11(1)	18(1)	18(1)	-2(1)	-1(1)	-2(1)
O(2)	11(1)	21(1)	16(1)	-4(1)	5(1)	-5(1)
O(3)	13(1)	18(1)	14(1)	1(1)	2(1)	1(1)
C(1)	12(1)	20(2)	10(1)	-1(1)	3(1)	-3(1)
C(2)	12(1)	19(2)	12(1)	-3(1)	2(1)	-1(1)
C(3)	12(1)	22(2)	15(2)	-4(1)	6(1)	2(1)
C(4)	12(2)	23(2)	24(2)	-5(1)	7(1)	-4(1)
C(5)	17(2)	17(2)	24(2)	-4(1)	8(1)	-4(1)
C(6)	12(1)	19(2)	14(2)	-3(1)	2(1)	-1(1)
C(7)	12(1)	18(2)	14(2)	-2(1)	2(1)	0(1)
C(8)	14(2)	19(2)	14(2)	-1(1)	3(1)	1(1)
C(9)	18(2)	22(2)	18(2)	1(1)	6(1)	-1(1)
C(10)	16(2)	20(2)	26(2)	-1(1)	4(1)	-2(1)
C(11)	14(2)	20(2)	18(2)	-6(1)	0(1)	-1(1)
C(12)	16(2)	21(2)	24(2)	-5(1)	3(1)	2(1)
C(13)	15(2)	21(2)	20(2)	-1(1)	2(1)	4(1)
C(14)	12(1)	21(2)	16(2)	-2(1)	1(1)	2(1)
C(15)	12(1)	20(2)	13(1)	-1(1)	3(1)	1(1)
C(16)	22(2)	24(2)	21(2)	4(1)	4(1)	1(1)
C(17)	14(2)	26(2)	40(2)	-7(2)	13(2)	-4(1)
C(18)	22(2)	69(3)	31(2)	-1(2)	14(2)	-5(2)
C(19)	17(2)	83(4)	23(2)	-3(2)	-3(2)	-11(2)
C(20)	18(2)	28(2)	172(7)	-15(3)	27(3)	-10(2)
C(21)	13(2)	17(2)	15(2)	-2(1)	2(1)	-2(1)
C(22)	16(2)	18(2)	32(2)	-2(1)	-1(1)	-1(1)
C(23)	15(2)	18(2)	51(3)	-6(2)	-7(2)	0(1)
C(24)	35(2)	22(2)	43(3)	-2(2)	-18(2)	2(2)
C(25)	39(2)	20(2)	21(2)	5(2)	-3(2)	-2(2)
C(26)	24(2)	18(2)	29(2)	-2(2)	-1(2)	-2(1)
C(27)	17(2)	21(2)	27(2)	-6(1)	1(1)	-3(1)
C(28)	14(2)	22(2)	17(2)	-2(1)	2(1)	-1(1)
C(29)	34(2)	22(2)	19(2)	1(1)	4(2)	-2(2)
C(30)	18(2)	25(2)	51(3)	-6(2)	9(2)	1(2)
C(31)	11(1)	17(2)	15(2)	1(1)	3(1)	0(1)
C(32)	11(1)	17(2)	17(2)	-1(1)	4(1)	0(1)
C(33)	14(2)	21(2)	18(2)	-7(1)	0(1)	-4(1)
C(34)	13(2)	23(2)	23(2)	-2(1)	6(1)	-4(1)
C(35)	14(1)	23(2)	18(2)	-2(1)	8(1)	-4(1)
C(36)	11(1)	17(1)	15(2)	-1(1)	3(1)	0(1)
C(37)	12(1)	20(2)	12(2)	-2(1)	2(1)	-1(1)
C(38)	12(2)	25(2)	18(2)	-4(1)	-1(1)	2(1)
C(39)	16(2)	34(2)	16(2)	-6(1)	-1(1)	2(1)
C(40)	20(2)	30(2)	29(2)	-15(2)	5(2)	-4(2)
C(41)	25(2)	19(2)	24(2)	-7(1)	6(2)	3(1)
C(42)	18(2)	29(2)	20(2)	-6(1)	3(1)	7(1)

C(43)	14(2)	26(2)	18(2)	-7(1)	6(1)	0(1)
C(44)	14(2)	21(2)	14(2)	-4(1)	2(1)	0(1)
C(45)	20(2)	19(2)	22(2)	-2(1)	4(1)	2(1)
C(46)	23(2)	32(2)	15(2)	-5(1)	5(1)	3(2)
C(47)	15(2)	29(2)	31(2)	-6(2)	10(2)	-7(1)
C(48)	18(2)	42(3)	54(3)	-1(2)	14(2)	-2(2)
C(49)	22(2)	43(2)	39(2)	0(2)	12(2)	-11(2)
C(50)	28(2)	48(3)	54(3)	-26(2)	18(2)	-22(2)
C(51)	13(1)	20(2)	12(1)	0(1)	5(1)	-1(1)
C(52)	14(2)	21(2)	14(2)	0(1)	3(1)	1(1)
C(53)	15(2)	29(2)	14(2)	0(1)	3(1)	0(1)
C(54)	15(2)	30(2)	36(2)	4(2)	14(2)	-2(2)
C(55)	20(2)	37(2)	18(2)	-8(2)	11(1)	-4(2)
C(56)	19(2)	32(2)	25(2)	-12(2)	10(1)	-3(2)
C(57)	16(2)	20(2)	23(2)	-4(1)	7(1)	-2(1)
C(58)	14(2)	19(2)	18(2)	0(1)	5(1)	0(1)
C(59)	16(2)	27(2)	18(2)	-3(1)	9(1)	-4(1)
C(60)	12(2)	27(2)	19(2)	-7(1)	4(1)	-4(1)
C(61)	16(2)	16(2)	15(2)	0(1)	1(1)	0(1)
C(62)	12(2)	22(2)	21(2)	2(1)	3(1)	0(1)
C(63)	15(2)	30(2)	38(2)	11(2)	8(2)	-1(1)
C(64)	22(2)	26(2)	48(3)	17(2)	10(2)	2(2)
C(65)	15(2)	24(2)	31(2)	7(2)	2(1)	4(1)
C(66)	12(2)	20(2)	18(2)	0(1)	3(1)	0(1)
C(67)	14(2)	24(2)	18(2)	2(1)	4(1)	2(1)
C(68)	18(2)	29(2)	15(2)	2(1)	7(1)	6(1)
C(69)	27(2)	35(2)	21(2)	3(2)	12(2)	12(2)
C(70)	19(2)	56(3)	24(2)	-1(2)	4(2)	16(2)
C(71)	16(2)	40(2)	32(2)	-4(2)	6(2)	-1(2)
C(72)	26(2)	46(3)	32(2)	2(2)	16(2)	3(2)
C(73)	26(2)	44(2)	17(2)	-1(2)	10(2)	3(2)
C(74)	21(2)	35(2)	15(2)	6(2)	3(1)	2(2)
C(75)	15(2)	33(2)	33(2)	-2(2)	5(2)	0(2)
C(76)	29(2)	37(2)	27(2)	-3(2)	11(2)	6(2)
C(77)	26(2)	39(3)	94(4)	43(3)	17(3)	5(2)
C(78)	47(4)	31(3)	36(3)	5(3)	8(3)	1(3)
C(79)	52(4)	38(4)	30(3)	14(3)	-3(3)	-9(3)
C(80)	39(4)	26(3)	53(5)	12(3)	-1(3)	-10(3)
C(78B)	26(7)	39(8)	67(11)	42(8)	15(7)	16(6)
C(79B)	42(8)	19(6)	34(7)	10(5)	24(6)	18(6)
C(80B)	70(15)	56(13)	77(16)	21(11)	42(13)	1(11)
C(81)	10(1)	20(2)	17(2)	2(1)	-1(1)	3(1)
C(82)	11(2)	23(2)	21(2)	-3(1)	3(1)	-1(1)
C(83)	13(2)	24(2)	36(2)	-2(2)	6(2)	-2(1)
C(84)	16(2)	34(2)	31(2)	10(2)	9(2)	5(2)
C(85)	18(2)	41(2)	18(2)	2(2)	7(1)	6(2)
C(86)	17(2)	36(2)	31(2)	0(2)	10(2)	5(2)
C(87)	10(2)	35(2)	28(2)	7(2)	2(1)	9(1)
C(88)	16(2)	27(2)	26(2)	9(2)	3(1)	3(1)
C(89)	14(2)	28(2)	18(2)	-3(1)	2(1)	4(1)
C(90)	13(2)	39(2)	25(2)	0(2)	4(1)	-1(2)
C(91)	76(2)	72(2)	118(3)	-4(2)	38(2)	3(2)
C(92)	76(2)	72(2)	118(3)	-4(2)	38(2)	3(2)

C(93)	76(2)	72(2)	118(3)	-4(2)	38(2)	3(2)
C(94)	76(2)	72(2)	118(3)	-4(2)	38(2)	3(2)
C(95)	76(2)	72(2)	118(3)	-4(2)	38(2)	3(2)
C(96)	76(2)	72(2)	118(3)	-4(2)	38(2)	3(2)

---

**Table 10:** Hydrogen coordinates ( $\times 10^4$ ) and isotropic displacement parameters ( $\text{\AA}^2 \times 10^3$ ) for  $\text{Lu}(\text{OAr}^*)_3$ .

	x	y	z	U(eq)
H(3A)	-1623	7200	5312	19
H(5A)	-764	5893	5603	23
H(8A)	1247	7540	5240	20
H(8B)	286	7593	4642	20
H(9A)	1275	8252	4733	23
H(10D)	1582	8738	5648	25
H(10E)	2026	8241	5871	25
H(11A)	1148	8495	6557	23
H(12A)	-546	8614	6112	26
H(12B)	-1	8964	5788	26
H(13A)	-1299	8605	4979	23
H(14A)	-1256	7804	4809	21
H(14B)	-1298	7899	5514	21
H(15A)	132	7845	6456	18
H(15B)	1147	7697	6400	18
H(16A)	-415	8374	4295	28
H(16B)	82	8819	4692	28
H(18A)	-2405	6435	6226	59
H(18B)	-3460	6469	5717	59
H(18C)	-2747	6896	5825	59
H(19A)	-2988	6927	4670	65
H(19B)	-3699	6499	4549	65
H(19C)	-2792	6486	4300	65
H(20A)	-2210	5724	5652	111
H(20B)	-2288	5746	4912	111
H(20C)	-3232	5792	5115	111
H(22A)	2366	6236	6441	29
H(22B)	2225	6254	5690	29
H(23A)	3465	5719	6199	39
H(24A)	2908	5518	7062	49
H(24B)	3100	5063	6716	49
H(25A)	1580	5007	6881	36
H(26A)	624	4834	5809	31
H(26B)	1687	4636	5951	31
H(27A)	1203	5020	4943	28
H(28A)	122	5554	5147	22
H(28B)	892	5826	4914	22
H(29A)	1228	5807	6847	31
H(29B)	341	5537	6365	31
H(30A)	2874	5073	5535	38
H(30B)	2531	5534	5131	38
H(33A)	5957	8434	7230	23
H(35A)	5869	7764	5624	21
H(38A)	5206	7781	8155	23
H(38B)	5750	8248	8112	23

H(39A)	5321	8253	9058	28
H(40A)	5303	8976	8562	32
H(40B)	4497	8966	8906	32
H(41A)	3842	9277	7856	28
H(42A)	2768	8858	8259	28
H(42B)	2460	8795	7497	28
H(43A)	2477	8068	7985	23
H(44A)	2911	8052	7037	20
H(44B)	3506	7668	7520	20
H(45A)	4807	8889	7345	25
H(45B)	3702	8805	6946	25
H(46A)	3938	7767	8703	28
H(46B)	3670	8230	8998	28
H(48A)	8433	8045	6719	56
H(48B)	7624	7690	6338	56
H(48C)	7786	7795	7078	56
H(49A)	7673	8632	5860	51
H(49B)	6557	8745	5692	51
H(49C)	6888	8257	5509	51
H(50A)	8008	8822	6962	63
H(50B)	7467	8582	7400	63
H(50C)	6914	8946	6867	63
H(52A)	2797	7596	5238	20
H(52B)	3276	7866	4786	20
H(53A)	1977	7399	4155	24
H(54A)	2830	7024	3513	31
H(54B)	3273	7525	3716	31
H(55A)	4546	6979	3948	29
H(56A)	4641	6378	4680	29
H(56B)	3652	6335	4100	29
H(57A)	3358	6244	5099	24
H(58A)	4653	6710	5728	20
H(58B)	3673	6862	5836	20
H(59A)	4822	7608	4674	23
H(59B)	5351	7160	5039	23
H(60A)	2104	6588	4248	24
H(60B)	2111	6804	4918	24
H(63A)	2066	5762	8452	33
H(65A)	4728	5519	8441	29
H(68A)	2220	7218	7795	24
H(68B)	1445	6975	7201	24
H(69A)	768	7640	7511	32
H(70A)	-651	7292	7597	40
H(70B)	-309	7030	7069	40
H(71A)	-676	6486	7757	36
H(72A)	-328	6951	8698	39
H(72B)	243	6476	8874	39
H(73A)	1294	7102	9318	35
H(74A)	2007	6449	9024	29
H(74B)	2551	6900	8916	29
H(75A)	585	6288	7341	33
H(75B)	776	6061	8033	33
H(76A)	559	7665	8537	36



H(76B)	1679	7634	8619	36
H(78A)	3183	4733	7824	59
H(78B)	3615	4394	8418	59
H(78C)	4285	4773	8255	59
H(79A)	3889	5227	9664	66
H(79B)	4682	5094	9341	66
H(79C)	4038	4704	9506	66
H(80A)	2043	5084	8902	65
H(80B)	2342	4582	8746	65
H(80C)	1942	4946	8181	65
H(78D)	2471	5333	9300	66
H(78E)	3591	5390	9676	66
H(78F)	3095	4900	9636	66
H(79D)	4763	5113	9331	44
H(79E)	4634	4786	8726	44
H(79F)	4320	4612	9317	44
H(80D)	1950	4916	8280	95
H(80E)	2592	4480	8583	95
H(80F)	2663	4706	7939	95
H(82A)	4885	6974	7878	23
H(82B)	5527	6790	8566	23
H(83A)	6486	7232	8090	29
H(84A)	5629	7067	6994	32
H(84B)	6746	6960	7139	32
H(85A)	5815	6342	6555	30
H(86A)	7345	6152	7302	33
H(86B)	6610	5739	7258	33
H(87A)	7448	5902	8355	30
H(88A)	6092	5976	8710	29
H(88B)	5841	5637	8108	29
H(89A)	4854	5901	7027	25
H(89B)	4463	6416	6912	25
H(90A)	7755	6690	8234	32
H(90B)	7282	6627	8791	32
H(91A)	4681	3596	7633	130
H(91B)	5244	3516	7131	130
H(91C)	4108	3589	6881	130
H(92A)	4293	4338	7237	104
H(92B)	5425	4269	7535	104
H(93A)	4366	4269	6221	104
H(93B)	5480	4153	6493	104
H(94A)	5851	4898	6812	104
H(94B)	4742	5026	6647	104
H(95A)	5645	4787	5721	104
H(95B)	4521	4873	5539	104
H(96A)	5242	5509	5274	130
H(96B)	5944	5555	5996	130
H(96C)	4819	5645	5833	130

**Table 11:** Atomic coordinates ( $\times 10^4$ ) and equivalent isotropic displacement parameters ( $\text{\AA}^2 \times 10^3$ ) for  $[\text{K}(\text{crypt})][\text{Lu}(\text{OAr}^*)_3] \cdot 3\text{Et}_2\text{O}$  (**4**).  $U(\text{eq})$  is defined as one third of the trace of the orthogonalized  $U^{ij}$  tensor.

	x	y	z	U(eq)
Lu(1)	5032(1)	5005(1)	7573(1)	14(1)
O(1)	6227(1)	5160(2)	7501(1)	15(1)
O(2)	3771(1)	6122(1)	7689(1)	14(1)
O(3)	5121(2)	3732(1)	7720(1)	15(1)
C(1)	7090(2)	4988(2)	7587(1)	13(1)
C(2)	7258(2)	5388(2)	8050(1)	13(1)
C(3)	8158(2)	5013(2)	8216(1)	16(1)
C(4)	8899(2)	4318(2)	7925(2)	18(1)
C(5)	8735(2)	4055(2)	7409(1)	17(1)
C(6)	7859(2)	4382(2)	7217(1)	14(1)
C(7)	6482(2)	6178(2)	8392(1)	13(1)
C(8)	6880(2)	6635(2)	8751(2)	19(1)
C(9)	6111(2)	7434(2)	9087(2)	20(1)
C(10)	5532(2)	7087(2)	9516(1)	21(1)
C(11)	5116(2)	6651(2)	9172(2)	21(1)
C(12)	4502(2)	7346(2)	8728(2)	25(1)
C(13)	5078(2)	7701(2)	8306(2)	24(1)
C(14)	5861(2)	6918(2)	7966(1)	20(1)
C(15)	5890(2)	5859(2)	8836(1)	17(1)
C(16)	5490(3)	8136(2)	8654(2)	26(1)
C(17)	9866(2)	3833(2)	8150(2)	22(1)
C(18)	10146(3)	2819(3)	8227(2)	36(1)
C(19)	10572(3)	3970(3)	7713(2)	43(1)
C(20)	9884(3)	4133(3)	8759(2)	42(1)
C(21)	7747(2)	4084(2)	6629(1)	14(1)
C(22)	8688(2)	3597(2)	6259(1)	20(1)
C(23)	8578(2)	3321(2)	5661(2)	24(1)
C(24)	8138(2)	2681(2)	5765(2)	24(1)
C(25)	7198(2)	3158(2)	6120(2)	21(1)
C(26)	6571(3)	4001(2)	5768(2)	25(1)
C(27)	7021(3)	4636(2)	5651(1)	22(1)
C(28)	7143(2)	4915(2)	6243(1)	18(1)
C(29)	7318(2)	3428(2)	6714(1)	17(1)
C(30)	7961(3)	4159(3)	5298(2)	26(1)
C(31)	3075(2)	6937(2)	7821(1)	13(1)
C(32)	2938(2)	7703(2)	7438(1)	14(1)
C(33)	2351(2)	8552(2)	7654(1)	17(1)
C(34)	1859(2)	8687(2)	8208(1)	17(1)
C(35)	1906(2)	7923(2)	8533(1)	15(1)
C(36)	2475(2)	7050(2)	8348(1)	14(1)
C(37)	3377(2)	7620(2)	6797(1)	13(1)
C(38)	3183(2)	6959(2)	6481(1)	15(1)
C(39)	3599(2)	6863(2)	5833(1)	18(1)
C(40)	4640(2)	6533(2)	5813(2)	24(1)

C(41)	4840(2)	7205(2)	6098(1)	21(1)
C(42)	4399(2)	8119(2)	5763(2)	23(1)
C(43)	3356(2)	8445(2)	5793(1)	18(1)
C(44)	2957(2)	8529(2)	6442(1)	18(1)
C(45)	4426(2)	7296(2)	6751(1)	16(1)
C(46)	3161(2)	7773(2)	5499(1)	20(1)
C(47)	1320(2)	9632(2)	8446(2)	22(1)
C(48)	728(3)	9647(3)	9031(2)	31(1)
C(49)	2008(3)	9966(3)	8558(2)	36(1)
C(50)	676(3)	10281(3)	8000(2)	33(1)
C(51)	2440(2)	6257(2)	8732(1)	13(1)
C(52)	1575(2)	6578(2)	9185(1)	18(1)
C(53)	1523(2)	5784(2)	9558(1)	20(1)
C(54)	2380(2)	5319(2)	9900(1)	21(1)
C(55)	3251(2)	4981(2)	9465(2)	20(1)
C(56)	3223(2)	4319(2)	9061(2)	21(1)
C(57)	2363(2)	4778(2)	8722(2)	21(1)
C(58)	2381(2)	5581(2)	8347(1)	17(1)
C(59)	3289(2)	5772(2)	9088(1)	16(1)
C(60)	1496(2)	5115(2)	9158(2)	23(1)
C(61)	4907(2)	3068(2)	7927(1)	13(1)
C(62)	4249(2)	2921(2)	7661(1)	14(1)
C(63)	3893(2)	2376(2)	7971(1)	16(1)
C(64)	4189(2)	1924(2)	8506(1)	17(1)
C(65)	4929(2)	1972(2)	8705(1)	16(1)
C(66)	5322(2)	2509(2)	8425(1)	13(1)
C(67)	3947(2)	3313(2)	7038(1)	14(1)
C(68)	4812(2)	3094(2)	6596(1)	16(1)
C(69)	4549(2)	3454(2)	5970(1)	20(1)
C(70)	3946(2)	4476(2)	5971(2)	21(1)
C(71)	3067(2)	4687(2)	6387(2)	20(1)
C(72)	2531(2)	4242(2)	6173(2)	22(1)
C(73)	3140(2)	3223(2)	6176(2)	21(1)
C(74)	3398(2)	2881(2)	6807(1)	18(1)
C(75)	3326(2)	4335(2)	7018(1)	16(1)
C(76)	4011(3)	3010(2)	5754(2)	23(1)
C(77)	3724(2)	1376(2)	8834(2)	24(1)
C(78)	3886(3)	599(3)	8453(2)	38(1)
C(79)	2685(3)	1975(3)	8929(2)	44(1)
C(80)	4102(4)	973(4)	9426(2)	56(2)
C(81)	6160(2)	2493(2)	8675(1)	13(1)
C(82)	6595(2)	1687(2)	9122(1)	17(1)
C(83)	7449(2)	1652(2)	9358(2)	20(1)
C(84)	7153(2)	2515(2)	9680(2)	21(1)
C(85)	6729(2)	3329(2)	9251(2)	21(1)
C(86)	7446(2)	3258(3)	8738(2)	25(1)
C(87)	7757(2)	2392(3)	8417(2)	24(1)
C(88)	6927(2)	2389(2)	8174(1)	20(1)
C(89)	5886(2)	3345(2)	9012(1)	17(1)
C(90)	8175(2)	1576(3)	8848(2)	25(1)
K(1)	-1759(1)	8596(1)	6701(1)	18(1)
O(4)	-3038(2)	7907(2)	6794(1)	24(1)
O(5)	-1167(2)	6761(2)	6483(1)	24(1)

O(6)	-2588(2)	10070(2)	5860(1)	26(1)
O(7)	-639(2)	9026(2)	5803(1)	26(1)
O(8)	-2455(2)	9673(2)	7685(1)	32(1)
O(9)	-600(2)	8337(2)	7554(1)	35(1)
N(1)	-3795(2)	9869(2)	6862(1)	22(1)
N(2)	280(2)	7329(2)	6491(1)	24(1)
C(91)	-4303(2)	9340(2)	7015(2)	26(1)
C(92)	-3949(2)	8507(3)	6662(2)	26(1)
C(93)	-2731(3)	7049(2)	6558(2)	26(1)
C(94)	-1793(3)	6432(2)	6749(2)	27(1)
C(95)	-238(3)	6133(3)	6568(2)	33(1)
C(96)	395(3)	6493(3)	6251(2)	30(1)
C(97)	-4092(2)	10397(2)	6314(2)	27(1)
C(98)	-3460(3)	10784(3)	6033(2)	32(1)
C(99)	-1954(3)	10400(3)	5614(2)	34(1)
C(100)	-1106(3)	9640(3)	5348(2)	35(1)
C(101)	166(3)	8285(3)	5571(2)	31(1)
C(102)	734(2)	7750(3)	6069(2)	27(1)
C(103)	-3952(3)	10458(2)	7347(2)	29(1)
C(104)	-3410(3)	9976(3)	7860(2)	31(1)
C(105)	-1909(3)	9281(3)	8167(2)	44(1)
C(106)	-922(3)	9028(3)	7961(2)	47(1)
C(107)	373(3)	7950(3)	7417(2)	36(1)
C(108)	679(2)	7132(3)	7062(2)	29(1)
O(10)	-2333(3)	7696(3)	4836(2)	72(1)
C(109)	-3741(4)	9054(5)	4788(3)	73(2)
C(110)	-2762(5)	8642(5)	4903(3)	77(2)
C(111)	-1391(4)	7261(5)	4946(3)	76(2)
C(112)	-974(6)	6255(5)	4859(4)	108(3)
O(11)	-882(3)	7597(3)	9133(2)	59(1)
C(113)	-817(4)	6686(4)	8371(2)	53(1)
C(114)	-1118(4)	6928(4)	9025(2)	53(1)
C(115)	-1182(4)	7893(4)	9700(2)	60(2)
C(116)	-884(5)	8554(6)	9821(3)	98(3)
O(12)	1494(3)	10761(3)	6516(2)	61(1)
C(117)	411(5)	10286(4)	6302(3)	75(2)
C(118)	573(4)	11076(4)	6399(3)	61(2)
C(119)	1688(6)	11428(5)	6680(3)	86(2)
C(120)	2680(7)	10984(6)	6849(4)	110(3)

---

**Table 12:** Bond lengths [Å] and angles [°] for [K(crypt)][Lu(OAr<sup>\*</sup>)<sub>3</sub>].3Et<sub>2</sub>O (**4**).

---

Lu(1)-O(2)	2.062(2)
Lu(1)-O(3)	2.069(2)
Lu(1)-O(1)	2.074(2)
O(1)-C(1)	1.344(4)
O(2)-C(31)	1.349(4)
O(3)-C(61)	1.342(4)
C(1)-C(2)	1.421(4)
C(1)-C(6)	1.433(4)
C(2)-C(3)	1.398(4)
C(2)-C(7)	1.543(4)
C(3)-C(4)	1.385(4)
C(4)-C(5)	1.394(5)
C(4)-C(17)	1.541(4)
C(5)-C(6)	1.393(4)
C(6)-C(21)	1.536(4)
C(7)-C(14)	1.541(4)
C(7)-C(15)	1.543(4)
C(7)-C(8)	1.548(4)
C(8)-C(9)	1.541(5)
C(9)-C(16)	1.525(5)
C(9)-C(10)	1.536(5)
C(10)-C(11)	1.521(5)
C(11)-C(12)	1.533(5)
C(11)-C(15)	1.537(4)
C(12)-C(13)	1.533(5)
C(13)-C(16)	1.522(5)
C(13)-C(14)	1.541(5)
C(17)-C(19)	1.516(5)
C(17)-C(20)	1.531(5)
C(17)-C(18)	1.542(5)
C(21)-C(29)	1.542(4)
C(21)-C(22)	1.550(4)
C(21)-C(28)	1.553(4)
C(22)-C(23)	1.538(5)
C(23)-C(24)	1.531(5)
C(23)-C(30)	1.539(5)
C(24)-C(25)	1.533(5)
C(25)-C(29)	1.531(4)
C(25)-C(26)	1.535(5)
C(26)-C(27)	1.538(5)
C(27)-C(30)	1.531(5)
C(27)-C(28)	1.536(5)
C(31)-C(36)	1.422(4)
C(31)-C(32)	1.427(4)
C(32)-C(33)	1.396(4)
C(32)-C(37)	1.536(4)
C(33)-C(34)	1.390(4)
C(34)-C(35)	1.393(4)
C(34)-C(47)	1.531(4)
C(35)-C(36)	1.397(4)

C(36)-C(51)	1.542(4)
C(37)-C(45)	1.539(4)
C(37)-C(38)	1.544(4)
C(37)-C(44)	1.546(4)
C(38)-C(39)	1.539(4)
C(39)-C(46)	1.527(4)
C(39)-C(40)	1.529(5)
C(40)-C(41)	1.526(5)
C(41)-C(42)	1.535(5)
C(41)-C(45)	1.548(4)
C(42)-C(43)	1.532(5)
C(43)-C(46)	1.533(5)
C(43)-C(44)	1.534(4)
C(47)-C(49)	1.526(5)
C(47)-C(50)	1.528(5)
C(47)-C(48)	1.542(5)
C(51)-C(59)	1.541(4)
C(51)-C(58)	1.542(4)
C(51)-C(52)	1.551(4)
C(52)-C(53)	1.540(4)
C(53)-C(54)	1.530(5)
C(53)-C(60)	1.531(5)
C(54)-C(55)	1.533(5)
C(55)-C(56)	1.529(5)
C(55)-C(59)	1.533(4)
C(56)-C(57)	1.528(5)
C(57)-C(60)	1.530(5)
C(57)-C(58)	1.535(4)
C(61)-C(62)	1.425(4)
C(61)-C(66)	1.428(4)
C(62)-C(63)	1.391(4)
C(62)-C(67)	1.549(4)
C(63)-C(64)	1.393(4)
C(64)-C(65)	1.385(4)
C(64)-C(77)	1.534(4)
C(65)-C(66)	1.397(4)
C(66)-C(81)	1.539(4)
C(67)-C(75)	1.538(4)
C(67)-C(68)	1.548(4)
C(67)-C(74)	1.549(4)
C(68)-C(69)	1.531(4)
C(69)-C(76)	1.534(5)
C(69)-C(70)	1.535(5)
C(70)-C(71)	1.535(5)
C(71)-C(72)	1.532(5)
C(71)-C(75)	1.538(4)
C(72)-C(73)	1.532(5)
C(73)-C(76)	1.530(5)
C(73)-C(74)	1.535(5)
C(77)-C(80)	1.523(5)
C(77)-C(79)	1.527(5)
C(77)-C(78)	1.536(6)
C(81)-C(89)	1.539(4)

C(81)-C(88)	1.548(4)
C(81)-C(82)	1.552(4)
C(82)-C(83)	1.536(5)
C(83)-C(90)	1.526(5)
C(83)-C(84)	1.528(5)
C(84)-C(85)	1.532(5)
C(85)-C(86)	1.524(5)
C(85)-C(89)	1.535(4)
C(86)-C(87)	1.527(5)
C(87)-C(88)	1.535(5)
C(87)-C(90)	1.536(5)
K(1)-O(9)	2.755(3)
K(1)-O(4)	2.800(2)
K(1)-O(8)	2.801(3)
K(1)-O(7)	2.841(3)
K(1)-O(5)	2.844(3)
K(1)-O(6)	2.881(3)
K(1)-N(1)	3.020(3)
K(1)-N(2)	3.029(3)
O(4)-C(92)	1.416(4)
O(4)-C(93)	1.424(4)
O(5)-C(95)	1.422(4)
O(5)-C(94)	1.423(4)
O(6)-C(98)	1.416(4)
O(6)-C(99)	1.424(4)
O(7)-C(100)	1.413(4)
O(7)-C(101)	1.417(4)
O(8)-C(105)	1.418(5)
O(8)-C(104)	1.420(5)
O(9)-C(106)	1.418(5)
O(9)-C(107)	1.422(5)
N(1)-C(97)	1.461(5)
N(1)-C(91)	1.465(4)
N(1)-C(103)	1.472(5)
N(2)-C(102)	1.466(5)
N(2)-C(108)	1.474(5)
N(2)-C(96)	1.476(5)
C(91)-C(92)	1.513(5)
C(93)-C(94)	1.499(5)
C(95)-C(96)	1.507(5)
C(97)-C(98)	1.509(5)
C(99)-C(100)	1.494(6)
C(101)-C(102)	1.506(5)
C(103)-C(104)	1.496(6)
C(105)-C(106)	1.494(7)
C(107)-C(108)	1.504(6)
O(10)-C(111)	1.416(7)
O(10)-C(110)	1.424(7)
C(109)-C(110)	1.474(9)
C(111)-C(112)	1.525(10)
O(11)-C(115)	1.379(6)
O(11)-C(114)	1.395(6)
C(113)-C(114)	1.544(7)

C(115)-C(116)	1.460(8)
O(12)-C(119)	1.390(7)
O(12)-C(118)	1.404(6)
C(117)-C(118)	1.505(9)
C(119)-C(120)	1.528(11)

O(2)-Lu(1)-O(3)	119.96(9)
O(2)-Lu(1)-O(1)	119.16(9)
O(3)-Lu(1)-O(1)	119.37(9)
C(1)-O(1)-Lu(1)	158.9(2)
C(31)-O(2)-Lu(1)	165.2(2)
C(61)-O(3)-Lu(1)	160.4(2)
O(1)-C(1)-C(2)	120.9(3)
O(1)-C(1)-C(6)	120.1(3)
C(2)-C(1)-C(6)	119.0(3)
C(3)-C(2)-C(1)	117.8(3)
C(3)-C(2)-C(7)	119.5(3)
C(1)-C(2)-C(7)	122.6(3)
C(4)-C(3)-C(2)	123.4(3)
C(3)-C(4)-C(5)	116.7(3)
C(3)-C(4)-C(17)	123.2(3)
C(5)-C(4)-C(17)	120.0(3)
C(6)-C(5)-C(4)	123.3(3)
C(5)-C(6)-C(1)	117.7(3)
C(5)-C(6)-C(21)	119.7(3)
C(1)-C(6)-C(21)	122.6(3)
C(14)-C(7)-C(2)	111.2(2)
C(14)-C(7)-C(15)	109.9(3)
C(2)-C(7)-C(15)	111.4(2)
C(14)-C(7)-C(8)	105.9(3)
C(2)-C(7)-C(8)	111.3(2)
C(15)-C(7)-C(8)	107.0(2)
C(9)-C(8)-C(7)	111.7(3)
C(16)-C(9)-C(10)	109.2(3)
C(16)-C(9)-C(8)	110.2(3)
C(10)-C(9)-C(8)	108.7(3)
C(11)-C(10)-C(9)	109.8(3)
C(10)-C(11)-C(12)	109.2(3)
C(10)-C(11)-C(15)	109.8(3)
C(12)-C(11)-C(15)	109.2(3)
C(13)-C(12)-C(11)	109.6(3)
C(16)-C(13)-C(12)	110.0(3)
C(16)-C(13)-C(14)	109.4(3)
C(12)-C(13)-C(14)	109.5(3)
C(13)-C(14)-C(7)	111.3(3)
C(11)-C(15)-C(7)	111.0(3)
C(13)-C(16)-C(9)	108.9(3)
C(19)-C(17)-C(20)	109.8(3)
C(19)-C(17)-C(4)	110.9(3)
C(20)-C(17)-C(4)	112.5(3)
C(19)-C(17)-C(18)	108.9(3)
C(20)-C(17)-C(18)	106.0(3)
C(4)-C(17)-C(18)	108.7(3)



C(6)-C(21)-C(29)	112.8(3)
C(6)-C(21)-C(22)	111.6(3)
C(29)-C(21)-C(22)	106.5(3)
C(6)-C(21)-C(28)	110.3(2)
C(29)-C(21)-C(28)	109.1(3)
C(22)-C(21)-C(28)	106.2(3)
C(23)-C(22)-C(21)	111.9(3)
C(24)-C(23)-C(22)	109.7(3)
C(24)-C(23)-C(30)	109.4(3)
C(22)-C(23)-C(30)	109.9(3)
C(23)-C(24)-C(25)	108.8(3)
C(29)-C(25)-C(24)	110.1(3)
C(29)-C(25)-C(26)	109.5(3)
C(24)-C(25)-C(26)	109.4(3)
C(25)-C(26)-C(27)	109.4(3)
C(30)-C(27)-C(28)	109.7(3)
C(30)-C(27)-C(26)	109.8(3)
C(28)-C(27)-C(26)	109.4(3)
C(27)-C(28)-C(21)	111.4(3)
C(25)-C(29)-C(21)	111.6(3)
C(27)-C(30)-C(23)	108.6(3)
O(2)-C(31)-C(36)	120.7(3)
O(2)-C(31)-C(32)	120.4(3)
C(36)-C(31)-C(32)	118.9(3)
C(33)-C(32)-C(31)	117.9(3)
C(33)-C(32)-C(37)	119.7(3)
C(31)-C(32)-C(37)	122.4(3)
C(34)-C(33)-C(32)	123.6(3)
C(33)-C(34)-C(35)	116.5(3)
C(33)-C(34)-C(47)	120.7(3)
C(35)-C(34)-C(47)	122.7(3)
C(34)-C(35)-C(36)	123.1(3)
C(35)-C(36)-C(31)	118.3(3)
C(35)-C(36)-C(51)	118.5(3)
C(31)-C(36)-C(51)	123.2(3)
C(32)-C(37)-C(45)	113.1(2)
C(32)-C(37)-C(38)	109.5(2)
C(45)-C(37)-C(38)	108.8(3)
C(32)-C(37)-C(44)	111.7(3)
C(45)-C(37)-C(44)	106.8(2)
C(38)-C(37)-C(44)	106.6(2)
C(39)-C(38)-C(37)	111.4(2)
C(46)-C(39)-C(40)	109.5(3)
C(46)-C(39)-C(38)	109.6(3)
C(40)-C(39)-C(38)	109.3(3)
C(41)-C(40)-C(39)	110.1(3)
C(40)-C(41)-C(42)	109.3(3)
C(40)-C(41)-C(45)	108.9(3)
C(42)-C(41)-C(45)	109.9(3)
C(43)-C(42)-C(41)	108.9(3)
C(42)-C(43)-C(46)	109.6(3)
C(42)-C(43)-C(44)	109.3(3)
C(46)-C(43)-C(44)	109.9(3)

C(43)-C(44)-C(37)	112.1(3)
C(37)-C(45)-C(41)	111.2(3)
C(39)-C(46)-C(43)	108.8(3)
C(49)-C(47)-C(50)	108.8(3)
C(49)-C(47)-C(34)	108.4(3)
C(50)-C(47)-C(34)	111.0(3)
C(49)-C(47)-C(48)	108.5(3)
C(50)-C(47)-C(48)	107.8(3)
C(34)-C(47)-C(48)	112.2(3)
C(59)-C(51)-C(58)	109.7(3)
C(59)-C(51)-C(36)	111.3(2)
C(58)-C(51)-C(36)	110.8(2)
C(59)-C(51)-C(52)	107.0(2)
C(58)-C(51)-C(52)	106.5(3)
C(36)-C(51)-C(52)	111.4(3)
C(53)-C(52)-C(51)	111.6(3)
C(54)-C(53)-C(60)	109.7(3)
C(54)-C(53)-C(52)	108.1(3)
C(60)-C(53)-C(52)	110.4(3)
C(53)-C(54)-C(55)	109.7(3)
C(56)-C(55)-C(59)	109.2(3)
C(56)-C(55)-C(54)	108.9(3)
C(59)-C(55)-C(54)	110.0(3)
C(57)-C(56)-C(55)	110.2(3)
C(56)-C(57)-C(60)	109.8(3)
C(56)-C(57)-C(58)	109.5(3)
C(60)-C(57)-C(58)	109.0(3)
C(57)-C(58)-C(51)	111.4(3)
C(55)-C(59)-C(51)	110.8(3)
C(57)-C(60)-C(53)	108.8(3)
O(3)-C(61)-C(62)	120.6(3)
O(3)-C(61)-C(66)	120.6(3)
C(62)-C(61)-C(66)	118.8(3)
C(63)-C(62)-C(61)	118.0(3)
C(63)-C(62)-C(67)	119.4(3)
C(61)-C(62)-C(67)	122.6(3)
C(62)-C(63)-C(64)	123.5(3)
C(65)-C(64)-C(63)	116.7(3)
C(65)-C(64)-C(77)	123.2(3)
C(63)-C(64)-C(77)	120.0(3)
C(64)-C(65)-C(66)	123.3(3)
C(65)-C(66)-C(61)	118.0(3)
C(65)-C(66)-C(81)	119.0(3)
C(61)-C(66)-C(81)	122.9(3)
C(75)-C(67)-C(68)	109.2(3)
C(75)-C(67)-C(62)	113.4(2)
C(68)-C(67)-C(62)	109.5(2)
C(75)-C(67)-C(74)	106.6(3)
C(68)-C(67)-C(74)	106.7(2)
C(62)-C(67)-C(74)	111.2(2)
C(69)-C(68)-C(67)	111.5(3)
C(68)-C(69)-C(76)	109.7(3)
C(68)-C(69)-C(70)	109.6(3)

C(76)-C(69)-C(70)	109.4(3)
C(69)-C(70)-C(71)	109.2(3)
C(72)-C(71)-C(70)	109.6(3)
C(72)-C(71)-C(75)	109.9(3)
C(70)-C(71)-C(75)	109.6(3)
C(71)-C(72)-C(73)	108.9(3)
C(76)-C(73)-C(72)	109.5(3)
C(76)-C(73)-C(74)	110.3(3)
C(72)-C(73)-C(74)	108.9(3)
C(73)-C(74)-C(67)	111.9(3)
C(71)-C(75)-C(67)	111.0(3)
C(73)-C(76)-C(69)	108.9(3)
C(80)-C(77)-C(79)	109.6(4)
C(80)-C(77)-C(64)	112.5(3)
C(79)-C(77)-C(64)	109.3(3)
C(80)-C(77)-C(78)	107.9(4)
C(79)-C(77)-C(78)	108.0(3)
C(64)-C(77)-C(78)	109.4(3)
C(66)-C(81)-C(89)	111.5(2)
C(66)-C(81)-C(88)	110.7(2)
C(89)-C(81)-C(88)	110.0(3)
C(66)-C(81)-C(82)	111.8(3)
C(89)-C(81)-C(82)	106.2(2)
C(88)-C(81)-C(82)	106.5(2)
C(83)-C(82)-C(81)	112.0(3)
C(90)-C(83)-C(84)	109.7(3)
C(90)-C(83)-C(82)	110.2(3)
C(84)-C(83)-C(82)	108.4(3)
C(83)-C(84)-C(85)	109.5(3)
C(86)-C(85)-C(84)	109.0(3)
C(86)-C(85)-C(89)	109.3(3)
C(84)-C(85)-C(89)	109.8(3)
C(85)-C(86)-C(87)	110.2(3)
C(86)-C(87)-C(88)	109.8(3)
C(86)-C(87)-C(90)	109.9(3)
C(88)-C(87)-C(90)	108.8(3)
C(87)-C(88)-C(81)	111.0(3)
C(85)-C(89)-C(81)	111.1(3)
C(83)-C(90)-C(87)	108.8(3)
O(9)-K(1)-O(4)	124.21(9)
O(9)-K(1)-O(8)	61.16(8)
O(4)-K(1)-O(8)	98.67(8)
O(9)-K(1)-O(7)	92.77(9)
O(4)-K(1)-O(7)	138.42(8)
O(8)-K(1)-O(7)	117.24(8)
O(9)-K(1)-O(5)	98.04(8)
O(4)-K(1)-O(5)	59.71(7)
O(8)-K(1)-O(5)	136.31(8)
O(7)-K(1)-O(5)	100.61(7)
O(9)-K(1)-O(6)	131.06(9)
O(4)-K(1)-O(6)	99.59(8)
O(8)-K(1)-O(6)	94.49(8)
O(7)-K(1)-O(6)	59.59(7)

O(5)-K(1)-O(6)	124.60(8)
O(9)-K(1)-N(1)	121.62(8)
O(4)-K(1)-N(1)	60.71(8)
O(8)-K(1)-N(1)	60.77(8)
O(7)-K(1)-N(1)	118.52(8)
O(5)-K(1)-N(1)	119.86(8)
O(6)-K(1)-N(1)	59.51(7)
O(9)-K(1)-N(2)	60.25(8)
O(4)-K(1)-N(2)	119.30(8)
O(8)-K(1)-N(2)	120.98(8)
O(7)-K(1)-N(2)	59.95(8)
O(5)-K(1)-N(2)	59.88(8)
O(6)-K(1)-N(2)	118.76(8)
N(1)-K(1)-N(2)	177.94(8)
C(92)-O(4)-C(93)	111.7(3)
C(92)-O(4)-K(1)	117.3(2)
C(93)-O(4)-K(1)	116.8(2)
C(95)-O(5)-C(94)	111.2(3)
C(95)-O(5)-K(1)	118.3(2)
C(94)-O(5)-K(1)	113.10(19)
C(98)-O(6)-C(99)	111.1(3)
C(98)-O(6)-K(1)	118.1(2)
C(99)-O(6)-K(1)	111.1(2)
C(100)-O(7)-C(101)	111.3(3)
C(100)-O(7)-K(1)	116.1(2)
C(101)-O(7)-K(1)	115.7(2)
C(105)-O(8)-C(104)	112.1(3)
C(105)-O(8)-K(1)	112.1(2)
C(104)-O(8)-K(1)	115.6(2)
C(106)-O(9)-C(107)	112.2(3)
C(106)-O(9)-K(1)	115.7(2)
C(107)-O(9)-K(1)	121.1(2)
C(97)-N(1)-C(91)	109.4(3)
C(97)-N(1)-C(103)	110.7(3)
C(91)-N(1)-C(103)	110.1(3)
C(97)-N(1)-K(1)	109.8(2)
C(91)-N(1)-K(1)	108.6(2)
C(103)-N(1)-K(1)	108.3(2)
C(102)-N(2)-C(108)	110.1(3)
C(102)-N(2)-C(96)	109.5(3)
C(108)-N(2)-C(96)	110.1(3)
C(102)-N(2)-K(1)	110.0(2)
C(108)-N(2)-K(1)	107.9(2)
C(96)-N(2)-K(1)	109.2(2)
N(1)-C(91)-C(92)	114.1(3)
O(4)-C(92)-C(91)	109.4(3)
O(4)-C(93)-C(94)	108.8(3)
O(5)-C(94)-C(93)	108.2(3)
O(5)-C(95)-C(96)	108.9(3)
N(2)-C(96)-C(95)	113.7(3)
N(1)-C(97)-C(98)	113.9(3)
O(6)-C(98)-C(97)	109.0(3)
O(6)-C(99)-C(100)	108.7(3)

O(7)-C(100)-C(99)	109.2(3)
O(7)-C(101)-C(102)	109.3(3)
N(2)-C(102)-C(101)	113.7(3)
N(1)-C(103)-C(104)	113.4(3)
O(8)-C(104)-C(103)	109.3(3)
O(8)-C(105)-C(106)	109.4(4)
O(9)-C(106)-C(105)	109.0(4)
O(9)-C(107)-C(108)	109.0(3)
N(2)-C(108)-C(107)	113.7(3)
C(111)-O(10)-C(110)	113.6(5)
O(10)-C(110)-C(109)	111.0(5)
O(10)-C(111)-C(112)	110.8(6)
C(115)-O(11)-C(114)	111.9(4)
O(11)-C(114)-C(113)	108.3(4)
O(11)-C(115)-C(116)	111.6(4)
C(119)-O(12)-C(118)	113.5(5)
O(12)-C(118)-C(117)	109.0(4)
O(12)-C(119)-C(120)	108.1(6)

---

**Table 13:** Anisotropic displacement parameters ( $\text{\AA}^2 \times 10^3$ ) for  $[\text{K}(\text{crypt})][\text{Lu}(\text{OAr}^*)_3] \cdot 3\text{Et}_2\text{O}$   
**(4).** The anisotropic displacement factor exponent takes the form:  $-2\pi^2 [h^2 a^{*2} U^{11} + \dots + 2 h k a^* b^* U^{12}]$ .

	$U^{11}$	$U^{22}$	$U^{33}$	$U^{23}$	$U^{13}$	$U^{12}$
Lu(1)	12(1)	11(1)	19(1)	1(1)	-2(1)	-5(1)
O(1)	13(1)	17(1)	14(1)	-2(1)	-2(1)	-7(1)
O(2)	13(1)	12(1)	14(1)	2(1)	-2(1)	-2(1)
O(3)	20(1)	13(1)	14(1)	3(1)	-5(1)	-9(1)
C(1)	13(1)	13(1)	14(1)	1(1)	-2(1)	-6(1)
C(2)	15(1)	13(2)	12(1)	0(1)	-1(1)	-6(1)
C(3)	19(2)	19(2)	13(2)	-2(1)	-5(1)	-10(1)
C(4)	14(2)	18(2)	21(2)	0(1)	-4(1)	-6(1)
C(5)	14(2)	17(2)	18(2)	-2(1)	0(1)	-5(1)
C(6)	16(2)	13(2)	15(2)	1(1)	-1(1)	-7(1)
C(7)	15(1)	13(2)	12(1)	0(1)	-2(1)	-5(1)
C(8)	19(2)	20(2)	18(2)	-2(1)	-2(1)	-9(1)
C(9)	23(2)	18(2)	20(2)	-4(1)	-2(1)	-9(1)
C(10)	22(2)	19(2)	16(2)	-1(1)	0(1)	-5(1)
C(11)	21(2)	22(2)	18(2)	-2(1)	5(1)	-10(1)
C(12)	14(2)	24(2)	31(2)	-9(2)	-3(1)	-2(1)
C(13)	26(2)	15(2)	19(2)	1(1)	-7(1)	1(1)
C(14)	24(2)	18(2)	13(2)	3(1)	-5(1)	-5(1)
C(15)	19(2)	14(2)	18(2)	0(1)	-2(1)	-8(1)
C(16)	33(2)	18(2)	21(2)	0(1)	-1(2)	-8(2)
C(17)	16(2)	22(2)	29(2)	-3(1)	-8(1)	-6(1)
C(18)	28(2)	27(2)	51(3)	6(2)	-17(2)	-7(2)
C(19)	19(2)	54(3)	54(3)	17(2)	-9(2)	-17(2)
C(20)	27(2)	45(3)	43(3)	-11(2)	-21(2)	-2(2)
C(21)	14(1)	14(2)	14(2)	-3(1)	-1(1)	-5(1)
C(22)	17(2)	23(2)	17(2)	-4(1)	1(1)	-7(1)
C(23)	23(2)	25(2)	20(2)	-9(1)	3(1)	-9(2)
C(24)	28(2)	21(2)	22(2)	-9(1)	-1(1)	-8(2)
C(25)	24(2)	18(2)	22(2)	-6(1)	-3(1)	-11(1)
C(26)	25(2)	29(2)	21(2)	-5(1)	-6(1)	-11(2)
C(27)	30(2)	20(2)	14(2)	0(1)	-4(1)	-8(2)
C(28)	21(2)	18(2)	14(2)	-1(1)	-1(1)	-8(1)
C(29)	19(2)	16(2)	14(2)	-1(1)	-1(1)	-7(1)
C(30)	34(2)	29(2)	14(2)	-4(1)	2(1)	-16(2)
C(31)	10(1)	14(2)	14(1)	0(1)	-4(1)	-4(1)
C(32)	15(1)	14(2)	14(2)	1(1)	-4(1)	-7(1)
C(33)	19(2)	13(2)	18(2)	2(1)	-5(1)	-6(1)
C(34)	15(2)	15(2)	20(2)	-3(1)	-3(1)	-5(1)
C(35)	15(2)	17(2)	14(2)	-2(1)	0(1)	-7(1)
C(36)	13(1)	14(2)	13(1)	2(1)	-5(1)	-6(1)
C(37)	14(1)	14(2)	12(1)	4(1)	-4(1)	-7(1)
C(38)	14(1)	16(2)	14(1)	2(1)	-2(1)	-7(1)
C(39)	24(2)	17(2)	12(2)	1(1)	-3(1)	-9(1)
C(40)	23(2)	23(2)	16(2)	0(1)	1(1)	-4(2)

C(41)	14(2)	30(2)	16(2)	5(1)	-1(1)	-9(1)
C(42)	24(2)	31(2)	18(2)	7(1)	-2(1)	-16(2)
C(43)	22(2)	16(2)	14(2)	6(1)	-4(1)	-8(1)
C(44)	19(2)	14(2)	17(2)	4(1)	-3(1)	-6(1)
C(45)	16(2)	19(2)	17(2)	5(1)	-5(1)	-10(1)
C(46)	20(2)	22(2)	15(2)	7(1)	-5(1)	-7(1)
C(47)	25(2)	17(2)	22(2)	-4(1)	4(1)	-9(1)
C(48)	33(2)	21(2)	33(2)	-7(2)	10(2)	-8(2)
C(49)	41(2)	29(2)	43(2)	-14(2)	4(2)	-20(2)
C(50)	36(2)	18(2)	36(2)	-2(2)	0(2)	-4(2)
C(51)	14(1)	14(2)	11(1)	1(1)	-1(1)	-7(1)
C(52)	16(2)	19(2)	17(2)	-1(1)	0(1)	-7(1)
C(53)	20(2)	20(2)	18(2)	1(1)	4(1)	-10(1)
C(54)	28(2)	20(2)	16(2)	2(1)	-2(1)	-13(2)
C(55)	20(2)	20(2)	18(2)	5(1)	-6(1)	-7(1)
C(56)	26(2)	15(2)	19(2)	2(1)	0(1)	-7(1)
C(57)	28(2)	20(2)	19(2)	-1(1)	-1(1)	-15(2)
C(58)	23(2)	17(2)	12(2)	0(1)	-4(1)	-10(1)
C(59)	17(2)	16(2)	16(2)	1(1)	-3(1)	-8(1)
C(60)	24(2)	25(2)	26(2)	5(1)	-5(1)	-16(2)
C(61)	14(1)	9(1)	13(1)	0(1)	-1(1)	-3(1)
C(62)	12(1)	11(1)	13(1)	0(1)	-2(1)	-1(1)
C(63)	15(2)	18(2)	17(2)	-1(1)	-2(1)	-8(1)
C(64)	18(2)	14(2)	19(2)	2(1)	1(1)	-8(1)
C(65)	20(2)	14(2)	12(1)	0(1)	-2(1)	-6(1)
C(66)	16(1)	11(1)	12(1)	-2(1)	-2(1)	-4(1)
C(67)	17(2)	12(2)	11(1)	0(1)	-3(1)	-5(1)
C(68)	18(2)	14(2)	12(1)	0(1)	-2(1)	-4(1)
C(69)	23(2)	20(2)	13(2)	0(1)	-4(1)	-6(1)
C(70)	26(2)	18(2)	17(2)	6(1)	-8(1)	-7(1)
C(71)	22(2)	12(2)	21(2)	2(1)	-9(1)	-3(1)
C(72)	22(2)	20(2)	22(2)	2(1)	-11(1)	-7(1)
C(73)	24(2)	18(2)	20(2)	-2(1)	-9(1)	-6(1)
C(74)	20(2)	16(2)	20(2)	0(1)	-7(1)	-7(1)
C(75)	14(2)	14(2)	17(2)	-1(1)	-3(1)	-4(1)
C(76)	30(2)	23(2)	14(2)	-3(1)	-7(1)	-8(2)
C(77)	24(2)	26(2)	24(2)	8(1)	-4(1)	-15(2)
C(78)	43(2)	28(2)	50(3)	7(2)	-2(2)	-24(2)
C(79)	30(2)	42(3)	55(3)	4(2)	15(2)	-18(2)
C(80)	76(4)	92(4)	33(2)	33(3)	-22(2)	-70(3)
C(81)	14(1)	12(1)	11(1)	2(1)	-3(1)	-4(1)
C(82)	20(2)	14(2)	17(2)	1(1)	-5(1)	-5(1)
C(83)	22(2)	16(2)	19(2)	4(1)	-6(1)	-7(1)
C(84)	23(2)	21(2)	18(2)	1(1)	-5(1)	-9(1)
C(85)	24(2)	19(2)	22(2)	-1(1)	-8(1)	-9(1)
C(86)	26(2)	29(2)	28(2)	9(2)	-10(2)	-19(2)
C(87)	15(2)	36(2)	18(2)	4(1)	-1(1)	-11(2)
C(88)	19(2)	26(2)	14(2)	1(1)	-2(1)	-10(1)
C(89)	17(2)	13(2)	20(2)	2(1)	-5(1)	-5(1)
C(90)	15(2)	28(2)	26(2)	-2(2)	-4(1)	-4(1)
K(1)	16(1)	16(1)	20(1)	0(1)	-3(1)	-7(1)
O(4)	22(1)	22(1)	31(1)	-3(1)	-3(1)	-13(1)
O(5)	20(1)	18(1)	33(1)	2(1)	-1(1)	-8(1)

O(6)	20(1)	22(1)	32(1)	6(1)	1(1)	-7(1)
O(7)	19(1)	25(1)	25(1)	4(1)	2(1)	-4(1)
O(8)	29(1)	30(2)	32(2)	-9(1)	-4(1)	-7(1)
O(9)	25(1)	40(2)	37(2)	-14(1)	-11(1)	-9(1)
N(1)	23(2)	17(1)	24(2)	2(1)	1(1)	-9(1)
N(2)	16(1)	22(2)	30(2)	0(1)	-3(1)	-6(1)
C(91)	18(2)	28(2)	29(2)	2(2)	1(1)	-9(2)
C(92)	23(2)	34(2)	28(2)	2(2)	-4(2)	-18(2)
C(93)	31(2)	26(2)	29(2)	-8(2)	0(2)	-18(2)
C(94)	30(2)	19(2)	36(2)	-2(2)	4(2)	-16(2)
C(95)	25(2)	18(2)	53(3)	4(2)	-9(2)	-6(2)
C(96)	20(2)	22(2)	42(2)	-5(2)	-1(2)	-4(2)
C(97)	18(2)	22(2)	32(2)	6(2)	-5(1)	-2(1)
C(98)	23(2)	19(2)	40(2)	9(2)	3(2)	-3(2)
C(99)	27(2)	28(2)	42(2)	17(2)	-3(2)	-11(2)
C(100)	26(2)	43(2)	27(2)	12(2)	2(2)	-11(2)
C(101)	21(2)	35(2)	28(2)	1(2)	4(2)	-8(2)
C(102)	14(2)	26(2)	35(2)	-5(2)	3(1)	-4(1)
C(103)	26(2)	21(2)	33(2)	-4(2)	1(2)	-6(2)
C(104)	30(2)	28(2)	30(2)	-11(2)	3(2)	-9(2)
C(105)	43(3)	41(3)	34(2)	-16(2)	-10(2)	-2(2)
C(106)	43(3)	46(3)	49(3)	-18(2)	-22(2)	-11(2)
C(107)	26(2)	48(3)	35(2)	-1(2)	-14(2)	-16(2)
C(108)	16(2)	32(2)	32(2)	3(2)	-4(1)	-5(2)
O(10)	77(3)	77(3)	77(3)	-8(2)	-17(2)	-43(3)
C(109)	59(4)	86(5)	71(4)	-24(4)	-4(3)	-26(3)
C(110)	94(5)	83(5)	70(4)	-28(4)	2(4)	-51(4)
C(111)	63(4)	108(6)	66(4)	4(4)	-18(3)	-45(4)
C(112)	123(7)	90(6)	141(8)	-5(5)	-61(6)	-63(6)
O(11)	69(3)	79(3)	46(2)	-4(2)	-3(2)	-48(2)
C(113)	54(3)	53(3)	52(3)	2(2)	-4(2)	-27(3)
C(114)	46(3)	55(3)	59(3)	3(3)	1(2)	-27(3)
C(115)	63(4)	75(4)	45(3)	-22(3)	24(3)	-38(3)
C(116)	117(6)	183(9)	47(3)	-43(4)	24(4)	-113(6)
O(12)	67(3)	55(2)	62(2)	-10(2)	-2(2)	-28(2)
C(117)	67(4)	72(4)	82(5)	16(3)	-29(3)	-26(3)
C(118)	48(3)	46(3)	64(4)	13(3)	-9(3)	-1(3)
C(119)	139(7)	72(5)	73(4)	-2(3)	0(4)	-74(5)
C(120)	158(9)	149(8)	87(5)	18(5)	-26(6)	-126(8)

---



**Table 14:** Hydrogen coordinates ( $\times 10^4$ ) and isotropic displacement parameters ( $\text{\AA}^2 \times 10^3$ ) for [K(crypt)][Lu(OAr<sup>\*</sup>)<sub>3</sub>] $\cdot$ 3Et<sub>2</sub>O (**4**).

	x	y	z	U(eq)
H(3A)	8267	5248	8544	19
H(5A)	9246	3632	7176	20
H(8A)	7281	6188	9036	23
H(8B)	7265	6850	8479	23
H(9A)	6392	7710	9315	24
H(10V)	5926	6643	9805	25
H(10W)	5033	7593	9735	25
H(12H)	4738	6429	9453	25
H(12F)	4233	7066	8500	31
H(12G)	3990	7850	8942	31
H(13A)	4674	8157	8019	28
H(14A)	6239	7146	7699	24
H(14B)	5593	6659	7720	24
H(15A)	5617	5567	8623	20
H(15B)	6288	5408	9122	20
H(16A)	4991	8643	8873	31
H(16B)	5853	8373	8381	31
H(18A)	10761	2502	8370	55
H(18B)	10157	2587	7846	55
H(18C)	9699	2722	8514	55
H(19A)	11178	3665	7868	65
H(19B)	10390	4614	7653	65
H(19C)	10603	3720	7335	65
H(20A)	10491	3760	8903	63
H(20B)	9408	4067	9036	63
H(20C)	9764	4764	8729	63
H(22A)	8985	3999	6189	24
H(22B)	9095	3054	6486	24
H(23A)	9199	3009	5438	28
H(24A)	8542	2128	5985	29
H(24B)	8058	2508	5381	29
H(25A)	6907	2743	6193	25
H(26A)	5961	4310	5994	30
H(26B)	6478	3829	5388	30
H(27A)	6614	5184	5419	27
H(28A)	6530	5249	6460	22
H(28B)	7437	5320	6167	22
H(29A)	7720	2883	6941	20
H(29B)	6710	3715	6945	20
H(30A)	8250	4568	5218	31
H(30B)	7885	3982	4915	31
H(33A)	2283	9065	7408	21
H(35A)	1532	7998	8897	18
H(38A)	3448	6363	6692	18
H(38B)	2508	7177	6494	18

H(39A)	3476	6419	5644	22
H(40A)	4926	5941	6026	28
H(40B)	4913	6460	5398	28
H(41A)	5522	6985	6081	25
H(42A)	4528	8559	5943	28
H(42B)	4664	8062	5346	28
H(43A)	3062	9045	5581	22
H(44A)	2280	8758	6460	21
H(44B)	3080	8970	6626	21
H(45A)	4724	6706	6966	20
H(45B)	4556	7728	6939	20
H(46A)	2487	7988	5508	24
H(46B)	3424	7714	5081	24
H(48A)	1131	9268	9333	47
H(48B)	294	9418	8969	47
H(48C)	385	10265	9161	47
H(49A)	2402	9573	8860	54
H(49B)	1673	10581	8695	54
H(49C)	2391	9959	8190	54
H(50A)	331	10878	8165	49
H(50B)	244	10062	7915	49
H(50C)	1041	10320	7634	49
H(52A)	1593	7003	9450	22
H(52B)	1014	6902	8972	22
H(53A)	957	6013	9843	24
H(54A)	2362	4807	10145	25
H(54B)	2391	5747	10166	25
H(55A)	3810	4672	9689	24
H(56A)	3782	4096	8778	25
H(56B)	3216	3797	9300	25
H(57A)	2353	4340	8459	25
H(58A)	1815	5888	8138	21
H(58B)	2918	5363	8047	21
H(59A)	3858	5550	8814	19
H(59B)	3310	6202	9349	19
H(60A)	1472	4603	9400	28
H(60B)	939	5412	8940	28
H(63A)	3423	2309	7808	19
H(65A)	5183	1621	9048	19
H(68A)	5181	3363	6726	19
H(68B)	5198	2435	6594	19
H(69A)	5122	3314	5698	24
H(70A)	3781	4713	5566	26
H(70B)	4292	4768	6105	26
H(71A)	2672	5353	6386	24
H(72A)	2358	4474	5769	26
H(72B)	1958	4383	6437	26
H(73A)	2792	2926	6043	26
H(74A)	3774	2220	6814	22
H(74B)	2828	3021	7073	22
H(75A)	2757	4475	7286	19
H(75B)	3653	4640	7159	19
H(76A)	3840	3242	5349	28

H(76B)	4399	2352	5745	28
H(78A)	3580	254	8659	57
H(78B)	4549	205	8385	57
H(78C)	3631	842	8073	57
H(79A)	2383	1619	9122	66
H(79B)	2441	2223	8547	66
H(79C)	2564	2467	9181	66
H(80A)	3798	617	9612	83
H(80B)	3985	1458	9683	83
H(80C)	4769	586	9363	83
H(82A)	6130	1737	9458	21
H(82B)	6772	1121	8927	21
H(83A)	7713	1122	9640	24
H(84A)	7694	2507	9836	25
H(84B)	6695	2556	10018	25
H(85A)	6536	3894	9461	25
H(86A)	7985	3263	8888	30
H(86B)	7179	3782	8458	30
H(87A)	8230	2352	8083	28
H(88A)	7129	1818	7977	24
H(88B)	6679	2888	7875	24
H(89A)	5605	3882	8745	20
H(89B)	5421	3388	9346	20
H(90A)	8373	1015	8641	30
H(90B)	8723	1559	9002	30
H(91A)	-4960	9726	6952	31
H(91B)	-4269	9158	7440	31
H(92A)	-4354	8211	6762	32
H(92B)	-3954	8675	6234	32
H(93A)	-2704	7105	6121	31
H(93B)	-3168	6802	6703	31
H(94A)	-1808	6415	7185	33
H(94B)	-1594	5816	6624	33
H(95A)	-93	5548	6411	40
H(95B)	-152	6040	6995	40
H(96A)	1042	6029	6275	36
H(96B)	281	6607	5828	36
H(97A)	-4718	10895	6396	33
H(97B)	-4133	10011	6028	33
H(98A)	-3726	11175	5684	38
H(98B)	-3389	11152	6319	38
H(99A)	-1791	10659	5927	41
H(99B)	-2236	10879	5308	41
H(10D)	-1279	9334	5071	42
H(10E)	-697	9872	5123	42
H(10F)	531	8502	5282	37
H(10G)	-8	7900	5364	37
H(10H)	1327	7275	5900	33
H(10I)	874	8151	6284	33
H(10J)	-4617	10744	7485	34
H(10K)	-3786	10942	7192	34
H(10L)	-3602	10386	8191	37
H(10M)	-3528	9457	7998	37

H(10N)	-1971	8741	8329	53
H(10O)	-2122	9715	8485	53
H(10P)	-866	9558	7769	56
H(10Q)	-546	8816	8303	56
H(10R)	684	7779	7786	43
H(10S)	541	8392	7186	43
H(10T)	1360	6843	6989	35
H(10U)	504	6698	7298	35
H(10A)	-4053	9671	4922	110
H(10B)	-4034	8705	5003	110
H(10C)	-3785	9061	4363	110
H(11M)	-2435	8914	4625	93
H(11N)	-2715	8765	5310	93
H(11O)	-1334	7363	5356	91
H(11P)	-1048	7521	4673	91
H(11A)	-375	5948	5023	162
H(11B)	-891	6147	4436	162
H(11C)	-1388	6021	5062	162
H(11D)	-954	6198	8291	79
H(11E)	-153	6492	8290	79
H(11F)	-1154	7214	8116	79
H(11S)	-1792	7145	9107	64
H(11T)	-803	6390	9286	64
H(11U)	-937	7375	9986	72
H(11V)	-1864	8166	9754	72
H(11G)	-751	8481	10235	147
H(11H)	-1374	9161	9747	147
H(11I)	-326	8464	9563	147
H(11J)	-231	10501	6219	112
H(11K)	533	9887	6657	112
H(11L)	826	9956	5966	112
H(11W)	443	11486	6043	74
H(11X)	154	11414	6737	74
H(11Y)	1256	11745	7020	103
H(11Z)	1618	11873	6347	103
H(12A)	2790	11418	7043	165
H(12B)	3108	10784	6493	165
H(12C)	2776	10466	7121	165



The following ALERTS were generated. Each ALERT has the format  
**test-name\_ALERT\_alert-type\_alert-level.**  
Click on the hyperlinks for more details of the test.

---

**Alert level B**

[PLAT213 ALERT 2 B](#) Atom C20 has ADP max/min Ratio ..... 4.1 prolat

**Author Response: ...The data set was weak (120 sec/frame scans) and SQUEEZE was employed. The Ueq for was slightly higher than that of other atoms of the tert-butyl group. Disorder was addressed where appropriate.**

---

**Alert level C**

[PLAT213 ALERT 2 C](#) Atom C78B has ADP max/min Ratio ..... 3.8 prolat

**Author Response: ...The data set was weak (120 sec/frame scans) and SQUEEZE was employed. The Ueq for was slightly higher than that of other atoms of the tert-butyl group. Disorder was addressed where appropriate.**

<a href="#">PLAT220 ALERT 2 C</a>	NonSolvent Resd 1 C Ueq(max)/Ueq(min) Range	5.3 Ratio
<a href="#">PLAT222 ALERT 3 C</a>	NonSolvent Resd 1 H Uiso(max)/Uiso(min) Range	6.2 Ratio
<a href="#">PLAT234 ALERT 4 C</a>	Large Hirshfeld Difference C77 --C78B .	0.17 Ang.
<a href="#">PLAT242 ALERT 2 C</a>	Low 'MainMol' Ueq as Compared to Neighbors of	C17 Check
<a href="#">PLAT906 ALERT 3 C</a>	Large K Value in the Analysis of Variance .....	3.010 Check

---

**Alert level G**

<a href="#">PLAT002 ALERT 2 G</a>	Number of Distance or Angle Restraints on AtSite	8 Note
<a href="#">PLAT083 ALERT 2 G</a>	SHELXL Second Parameter in WGHT Unusually Large	32.40 Why ?
<a href="#">PLAT171 ALERT 4 G</a>	The CIF-Embedded .res File Contains EADP Records	1 Report
<a href="#">PLAT172 ALERT 4 G</a>	The CIF-Embedded .res File Contains DFIX Records	6 Report
<a href="#">PLAT230 ALERT 2 G</a>	Hirshfeld Test Diff for C77 --C78 .	14.7 s.u.
<a href="#">PLAT230 ALERT 2 G</a>	Hirshfeld Test Diff for C77 --C79 .	8.0 s.u.
<a href="#">PLAT300 ALERT 4 G</a>	Atom Site Occupancy of C78 Constrained at	0.7 Check
<a href="#">PLAT300 ALERT 4 G</a>	Atom Site Occupancy of C79 Constrained at	0.7 Check
<a href="#">PLAT300 ALERT 4 G</a>	Atom Site Occupancy of C80 Constrained at	0.7 Check
<a href="#">PLAT300 ALERT 4 G</a>	Atom Site Occupancy of C78B Constrained at	0.3 Check
<a href="#">PLAT300 ALERT 4 G</a>	Atom Site Occupancy of C79B Constrained at	0.3 Check
<a href="#">PLAT300 ALERT 4 G</a>	Atom Site Occupancy of C80B Constrained at	0.3 Check
<a href="#">PLAT300 ALERT 4 G</a>	Atom Site Occupancy of H78A Constrained at	0.7 Check
<a href="#">PLAT300 ALERT 4 G</a>	Atom Site Occupancy of H78B Constrained at	0.7 Check
<a href="#">PLAT300 ALERT 4 G</a>	Atom Site Occupancy of H78C Constrained at	0.7 Check
<a href="#">PLAT300 ALERT 4 G</a>	Atom Site Occupancy of H79A Constrained at	0.7 Check
<a href="#">PLAT300 ALERT 4 G</a>	Atom Site Occupancy of H79B Constrained at	0.7 Check
<a href="#">PLAT300 ALERT 4 G</a>	Atom Site Occupancy of H79C Constrained at	0.7 Check
<a href="#">PLAT300 ALERT 4 G</a>	Atom Site Occupancy of H80A Constrained at	0.7 Check
<a href="#">PLAT300 ALERT 4 G</a>	Atom Site Occupancy of H80B Constrained at	0.7 Check
<a href="#">PLAT300 ALERT 4 G</a>	Atom Site Occupancy of H80C Constrained at	0.7 Check
<a href="#">PLAT300 ALERT 4 G</a>	Atom Site Occupancy of H78D Constrained at	0.3 Check
<a href="#">PLAT300 ALERT 4 G</a>	Atom Site Occupancy of H78E Constrained at	0.3 Check
<a href="#">PLAT300 ALERT 4 G</a>	Atom Site Occupancy of H78F Constrained at	0.3 Check
<a href="#">PLAT300 ALERT 4 G</a>	Atom Site Occupancy of H79D Constrained at	0.3 Check
<a href="#">PLAT300 ALERT 4 G</a>	Atom Site Occupancy of H79E Constrained at	0.3 Check

PLAT300	ALERT 4	G	Atom Site Occupancy of H79F	Constrained at	0.3	Check
PLAT300	ALERT 4	G	Atom Site Occupancy of H80D	Constrained at	0.3	Check
PLAT300	ALERT 4	G	Atom Site Occupancy of H80E	Constrained at	0.3	Check
PLAT300	ALERT 4	G	Atom Site Occupancy of H80F	Constrained at	0.3	Check
PLAT301	ALERT 3	G	Main Residue Disorder .....(Resd 1 )		3%	Note
PLAT606	ALERT 4	G	Solvent Accessible VOID(S) in Structure .....			! Info
PLAT794	ALERT 5	G	Tentative Bond Valency for Lu1 (III) .		3.48	Info
PLAT860	ALERT 3	G	Number of Least-Squares Restraints .....		18	Note
PLAT869	ALERT 4	G	ALERTS Related to the Use of SQUEEZE Suppressed			! Info
PLAT978	ALERT 2	G	Number C-C Bonds with Positive Residual Density.		6	Info

---

0 **ALERT level A** = Most likely a serious problem - resolve or explain  
1 **ALERT level B** = A potentially serious problem, consider carefully  
6 **ALERT level C** = Check. Ensure it is not caused by an omission or oversight  
36 **ALERT level G** = General information/check it is not something unexpected

0 ALERT type 1 CIF construction/syntax error, inconsistent or missing data  
9 ALERT type 2 Indicator that the structure model may be wrong or deficient  
4 ALERT type 3 Indicator that the structure quality may be low  
29 ALERT type 4 Improvement, methodology, query or suggestion  
1 ALERT type 5 Informative message, check

---

It is advisable to attempt to resolve as many as possible of the alerts in all categories. Often the minor alerts point to easily fixed oversights, errors and omissions in your CIF or refinement strategy, so attention to these fine details can be worthwhile. In order to resolve some of the more serious problems it may be necessary to carry out additional measurements or structure refinements. However, the purpose of your study may justify the reported deviations and the more serious of these should normally be commented upon in the discussion or experimental section of a paper or in the "special\_details" fields of the CIF. checkCIF was carefully designed to identify outliers and unusual parameters, but every test has its limitations and alerts that are not important in a particular case may appear. Conversely, the absence of alerts does not guarantee there are no aspects of the results needing attention. It is up to the individual to critically assess their own results and, if necessary, seek expert advice.

### Publication of your CIF in IUCr journals

A basic structural check has been run on your CIF. These basic checks will be run on all CIFs submitted for publication in IUCr journals (*Acta Crystallographica*, *Journal of Applied Crystallography*, *Journal of Synchrotron Radiation*); however, if you intend to submit to *Acta Crystallographica Section C* or *E* or *IUCrData*, you should make sure that full publication checks are run on the final version of your CIF prior to submission.

### Publication of your CIF in other journals

Please refer to the *Notes for Authors* of the relevant journal for any special instructions relating to CIF submission.

---

**PLATON version of 05/12/2020; check.def file version of 05/12/2020**





The following ALERTS were generated. Each ALERT has the format  
**test-name\_ALERT\_alert-type\_alert-level.**  
Click on the hyperlinks for more details of the test.

 **Alert level A**

[PLAT971 ALERT 2 A](#) Check Calcd Resid. Dens. 0.85A From Lu1 4.35 eA-3

**Author Response: ...Residual density was observed near the Lu atom.  
Neither disorder nor alternative absorption corrections improved the model.**

 **Alert level B**

[PLAT094 ALERT 2 B](#) Ratio of Maximum / Minimum Residual Density .... 5.04 Report

**Author Response: ...The Max/min density resulted from the high residual density near the Lu atom.**


 **Alert level C**

<a href="#">PLAT220 ALERT 2 C</a>	NonSolvent Resd 1 C Ueq(max)/Ueq(min) Range	4.3 Ratio
<a href="#">PLAT222 ALERT 3 C</a>	NonSolvent Resd 1 H Uiso(max)/Uiso(min) Range	4.6 Ratio
<a href="#">PLAT244 ALERT 4 C</a>	Low 'Solvent' Ueq as Compared to Neighbors of	C115 Check
<a href="#">PLAT410 ALERT 2 C</a>	Short Intra H...H Contact H3A ..H8A .	1.97 Ang.
	x,y,z = 1_555	Check
<a href="#">PLAT410 ALERT 2 C</a>	Short Intra H...H Contact H35A ..H52A .	1.97 Ang.
	x,y,z = 1_555	Check
<a href="#">PLAT911 ALERT 3 C</a>	Missing FCF Refl Between Thmin & STh/L= 0.600	8 Report
<a href="#">PLAT971 ALERT 2 C</a>	Check Calcd Resid. Dens. 2.13A From Lu1	1.76 eA-3

**Author Response: ...Residual density was observed near the Lu atom.  
Neither disorder nor alternative absorption corrections improved the model.**

[PLAT971 ALERT 2 C](#) Check Calcd Resid. Dens. 0.91A From Lu1 1.52 eA-3

**Author Response: ...Residual density was observed near the Lu atom.  
Neither disorder nor alternative absorption corrections improved the model.**

 **Alert level G**

<a href="#">PLAT042 ALERT 1 G</a>	Calc. and Reported MoietyFormula Strings Differ	Please Check
<a href="#">PLAT083 ALERT 2 G</a>	SHELXL Second Parameter in WGHT Unusually Large	8.50 Why ?
<a href="#">PLAT790 ALERT 4 G</a>	Centre of Gravity not Within Unit Cell: Resd. #	2 Note
	C18 H36 K N2 O6	
<a href="#">PLAT790 ALERT 4 G</a>	Centre of Gravity not Within Unit Cell: Resd. #	3 Note
	C4 H10 O	
<a href="#">PLAT794 ALERT 5 G</a>	Tentative Bond Valency for Lu1 (III) .	2.30 Info
<a href="#">PLAT910 ALERT 3 G</a>	Missing # of FCF Reflection(s) Below Theta(Min).	1 Note

PLAT912	ALERT 4 G	Missing # of FCF Reflections Above STh/L= 0.600	14	Note
PLAT933	ALERT 2 G	Number of OMIT Records in Embedded .res File ...	8	Note
PLAT941	ALERT 3 G	Average HKL Measurement Multiplicity .....	4.5	Low
PLAT978	ALERT 2 G	Number C-C Bonds with Positive Residual Density.	1	Info

- 
- 1 **ALERT level A** = Most likely a serious problem - resolve or explain
  - 1 **ALERT level B** = A potentially serious problem, consider carefully
  - 8 **ALERT level C** = Check. Ensure it is not caused by an omission or oversight
  - 10 **ALERT level G** = General information/check it is not something unexpected
- 
- 1 ALERT type 1 CIF construction/syntax error, inconsistent or missing data
  - 10 ALERT type 2 Indicator that the structure model may be wrong or deficient
  - 4 ALERT type 3 Indicator that the structure quality may be low
  - 4 ALERT type 4 Improvement, methodology, query or suggestion
  - 1 ALERT type 5 Informative message, check
- 

It is advisable to attempt to resolve as many as possible of the alerts in all categories. Often the minor alerts point to easily fixed oversights, errors and omissions in your CIF or refinement strategy, so attention to these fine details can be worthwhile. In order to resolve some of the more serious problems it may be necessary to carry out additional measurements or structure refinements. However, the purpose of your study may justify the reported deviations and the more serious of these should normally be commented upon in the discussion or experimental section of a paper or in the "special\_details" fields of the CIF. checkCIF was carefully designed to identify outliers and unusual parameters, but every test has its limitations and alerts that are not important in a particular case may appear. Conversely, the absence of alerts does not guarantee there are no aspects of the results needing attention. It is up to the individual to critically assess their own results and, if necessary, seek expert advice.

### Publication of your CIF in IUCr journals

A basic structural check has been run on your CIF. These basic checks will be run on all CIFs submitted for publication in IUCr journals (*Acta Crystallographica*, *Journal of Applied Crystallography*, *Journal of Synchrotron Radiation*); however, if you intend to submit to *Acta Crystallographica Section C* or *E* or *IUCrData*, you should make sure that full publication checks are run on the final version of your CIF prior to submission.

### Publication of your CIF in other journals

Please refer to the *Notes for Authors* of the relevant journal for any special instructions relating to CIF submission.

---

**PLATON version of 05/12/2020; check.def file version of 05/12/2020**